AN ABSTRACT OF THE DISSERTATION OF

Ferhat Yıldırım for the degree of Doctor of Philosophy in
Electrical and Computer Engineering presented on September 23, 2009.

Title: Directional 60 GHz Communication Networks

Abstract approved: _____

Dr. Huaping Liu

It is well known that multipath effects cause inter-symbol interference (ISI) for high-speed signaling and ultimately limit the achievable data rate at any frequency band. In this thesis, we study several different methods to tackle this issue and provide solutions for establishing efficient wireless links that can provide several Gbps data rate. Specifically, we show that proper choice of polarization, when used with the proposed topology detection algorithm reduces the multipath in 60 GHz wireless channel and increases the error-performance of the network. We also develop a direction-detection algorithm for directional communications in 60 GHz, which is proven to be effective in reducing multipath and increasing spatial diversity. Finally, we propose a double directional channel model for 60 GHz channel as a modification to IEEE 802.15.3c channel model to include the effects of directional antennas both on the transmitter and the receiver side.

Directional 60 GHz Communication Networks

by

Ferhat Yıldırım

A DISSERTATION

submitted to

Oregon State University

in partial fulfillment of
the requirements for the
degree of

Doctor of Philosophy

Presented September 23, 2009
Commencement June 2010

Doctor of Philosophy dissertation of Ferhat Yıldırım presented on September 23, 2009.

APPROVED:

Major Professor, representing Electrical and Computer Engineering

---

Director of the School of Electric Engineering and Computer Science

---

Dean of the Graduate School

I understand that my dissertation will become part of the permanent collection of Oregon State University libraries. My signature below authorizes release of my dissertation to any reader upon request.

Ferhat Yıldırım, Author

ACKNOWLEDGEMENTS

I would like to express my sincere gratitude to my supervisor, Prof. Huaping Liu, for his guidance, motivation, understanding and support.

I also would like to thank to the members of my thesis committee for their valuable comments and inputs.

I also thank the members of the OSU Wireless Communication group for their cooperation and support.

CONTRIBUTION OF AUTHORS

Dr. Ali Sadri of Intel Corporation assisted in the redaction of Chapter 2 with his extensive knowledge in IEEE 802.15.3c standard. He provided insightful feedback to our theoretical derivation of the channel based on his previous measurement results of 60 GHz channel.

TABLE OF CONTENTS

TABLE OF CONTENTS (Continued)

TABLE OF CONTENTS (Continued)

LIST OF FIGURES

LIST OF FIGURES (Continued)

LIST OF FIGURES (Continued)

LIST OF TABLES

LIST OF APPENDIX FIGURES

Introduction

In the recent years, we have observed an ever growing demand for wireless access to information and entertainment from consumers, industry and government. Although both mobile cellular networks with recent improvements in third and forth generation systems and wireless local area networks provide broadband access to information networks, these systems can not compete with the wired systems and their several Gbps bandwidth capability. 60 GHz wireless networks come into the picture at this point by providing wireless access at Gbps order as an alternative to wired systems such as gigabit ethernet and HDMI [1]. With their ultra-high speed access, and large and unlicensed spectrum, 60 GHz wireless networks pave the road to a wireless future.

60 GHz wireless networks, although recently become a hot research topic, have been used by military for several decades in satellite-to-satellite communications. Electromagnetic waves in the 60 GHz band has an additional attenuation due to oxygen atoms in the atmosphere; therefore, it is highly inefficient to have a 60 GHz link between earth station and satellite due to the oxygen content of the atmosphere, especially the ozone layer. However, military used this for establishing secure links between satellites, where earth based eavesdropping is almost impossible.

Military applications prefer the 60 GHz spectrum due to its secure nature

rather than its high data rate capacity; however, due to overwhelming demand for high-speed data access and exhaustion of license-free spectrum, FCC and similar government bodies around the world, set aside a 5-7 GHz (depending on the country) spectrum centered around 60 GHz for license-free wireless communications. After the liberation of this spectrum, IEEE 802.15.3c has been formed to create a standard for physical (PHY) and MAC layers, which is in its final stages as of writing of this thesis.

In this thesis, I present the research I have done as part of my graduate study in the area of 60 GHz wireless networks. My research is based on the standard that is proposed by IEEE 802.15.3c Task Group. During my research, I proposed several modifications to the 60 GHz channel model, analyzed and solved practical issues, studied directional communications and observed the network characteristics of directional communications in 60 GHz spectrum. Each chapter of this thesis consists of a scholarly manuscript, several of which are published in international, peer-reviewed journals or proceedings; remaining were submitted for review.

This introduction chapter serves as a review of 60 GHz spectrum, its electromagnetic properties, the proposed channel model and usage models. I also try to link the distinct chapters of this thesis together so that reader can understand the logical flow of the progress.

1.1 60 GHz Channel Properties

One of the most unique characteristics of electromagnetic waves in the 60 GHz band is their attenuation due to oxygen atoms. This attenuation is 10–15 dB/km, but can have an additional attenuation up to 18 dB/km in the presence of rain [2]. Such attenuation is insignificant for indoor communications though.

In addition to oxygen absorption, the free space loss at 60 GHz is significantly higher when compared to lower frequency bands. Moreover, in 60 GHz band, electromagnetic waves lose their ability of diffraction (i.e., bend around the edges of objects) and scattering, and face increased attenuation for penetration [3]. These properties draw a very different picture for the channel in the 60 GHz spectrum when compared with the lower frequency wireless networks. For one, shadowing is a critical issue since it is difficult for the electromagnetic waves to penetrate through or diffract around the obstacles. This makes NLOS communication a challenging task for the 60 GHz wireless networks. However, these unique characteristics also provide some advantages such as security and less interference. Due to the increased material attenuation, walls in an indoor environment may act as cell boundaries. A concrete wall of 15 cm thick can introduce an attenuation as high as 36 dB [4], practically securing the wireless signals within the room. These pico-cells are secure for both intrusions and interference from nearby cells. Moreover, reduced interference enables spectrum reuse in neighboring cells and increases the performance of each cell.

Another significant difference of 60 GHz channel is its low delay spread, which

arises from the confinement of electromagnetic waves within a small room as well as lower number of multipath due to reduced diffraction, scattering and penetration. In 60 GHz channel, the rms delay spread for a typical indoor environment can vary from a few nanoseconds to 100 nanoseconds if omnidirectional antennas are used, and can be reduced down to a few nanoseconds if directional transmission is employed [5, 6].

1.2 IEEE 802.15.3c Standard

Under the IEEE 802.15.3 High Rate Task Group for Wireless Personal Area Networks (WPAN), an alternative Task Group (TG3c) started working on a physical layer (PHY) standard for 60 GHz channel that would enable wireless communications with over 2 Gbps data rate [7]. Along with an alternative PHY standard, an alternative medium access control (MAC) layer standard for higher frequency networks are also being developed for the IEEE 802.15.3c.

A piconet structure has been assumed for IEEE 802.15.3 WPANs. In such a network, any device can be designated as a PicoNet Controller (PNC) that serves as a central hub to other slave devices [8]. Task Group 3c proposes a set of usage models (UM) for applications of 60 GHz wireless networks that are foreseen to be used in practice [9]. These models are presented in Fig. 1.1. Two of the five usage models are designated as mandatory (UM1 and UM5), which consider only a single link between two devices, where directional information is obtained mostly by external means.

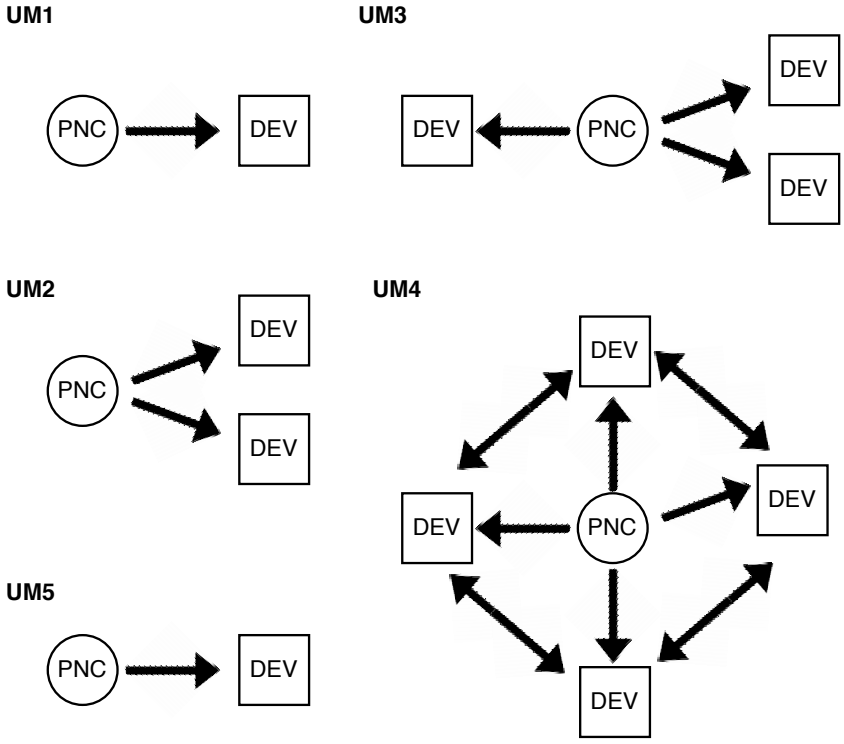

Figure 1.1: Usage models as defined in IEEE 802.15.3c [9].

These models are summarized as follows:

- *UM1*: Wireless streaming of uncompressed high-definition video from a source (set-top box, DVD player, game console, etc.) to a high-definition display device. The nodes are fixed, however the link can be LOS or NLOS, and random shadowing caused by human body is possible. The separation between nodes are 5–10 meters in a typical residential environment. Typical required data rate is 3.56 Gbps for a 1080p (1920x1080 pixels, progressive) image with a color depth 24 bit and 60 Hz refresh rate. This usage model is

designated as mandatory.

- *UM2*: Wireless streaming of uncompressed high-definition video from a source to multiple display devices, which are separated by 5 meters. The nodes are fixed, one display has a LOS with the source and the other ones are NLOS, and random shadowing caused by human body is possible. Video streams to each display are assumed to have a rate of 0.62 Gbps, resolution of 480p (640x480 pixels, progressive), color depth of 24 bit, and 60 Hz refresh. This usage model is designated as optional.

- *UM3*: Wireless personal area network of a typical office setting. A high-definition display device, which is separated from the computer by 1 meter, has similar link characteristics as UM1. The printer, which has a NLOS link to the computer, is separated by 5 meters. The external storage is assumed to have a LOS link to the computer with 0.25 Gbps link in both directions. This usage model is designated as optional.

- *UM4*: A wireless ad-hoc network setup in a conference room setup with a central control hub and a projector display device. Several computer nodes are available that are assumed to be 3 meters apart from the central hub. The link characteristics between a node and the display device are similar to UM1. A data rate of 0.125 Gbps is assumed between the controller hub and a computer node in both directions. The data rate between the computer nodes is assumed to be 0.0416 Gbps for a separation of 1 meter. In this scenario, all links are assumed to have a LOS link with the hub. This usage

model is designated as optional.

- *UM5*: Wireless data download from kiosk to a handheld device over a LOS link with a burst speed of up to 2 Gbps. The user needs to manually adjust the direction of the antennas; hence no neighbor discovery is necessary. This usage model is designated as mandatory.

1.2.1 Channel Model

The model proposed by IEEE 802.15.3c Task Group [7] is based on the well-known ToA Saleh-Valenzuela multipath model [10], whose channel impulse response is expressed as

$$h(t) = \sum_{l=0}^{L-1} \sum_{k=0}^{K_l-1} \alpha_{k,l} \delta(t - T_l - \tau_{k,l}) \tag{1.1}$$

where L is the number of clusters, K_l is the number of rays in the lth cluster, $a_{k,l}$ is the gain coefficient of the kth ray in the lth cluster, T_l is the arrival time of the first ray in the lth cluster, and $\tau_{k,l}$ is the delay of the kth ray within the lth cluster relative to the first arrival path of that cluster. The delay of the first ray received, i.e., T_0, is assumed to be zero, as well as the reference point in each cluster, i.e., $\tau_{0,l} = 0$. The delays of each cluster and each ray within a cluster are assumed to

follow the Poisson distribution given by

$$p(T_l|T_{l-1}) = \Lambda \exp(-\Lambda(T_l - T_{l-1})), l > 0 \tag{1.2a}$$

$$p(\tau_{k,l}|\tau_{(k-1),l}) = \lambda \exp(-\lambda(\tau_{k,l} - \tau_{(k-1),l})), k > 0 \tag{1.2b}$$

where Λ and λ correspond to cluster and ray arrival rate, respectively. The gain coefficient $\alpha_{k,l}$ is defined as

$$\alpha_{k,l} = p_{k,l}\beta_{k,l} \tag{1.3}$$

where $p_{k,l} = \pm 1$ with equal probability represents the inversion of phase after reflection. In the original S-V model, the amplitude of gain coefficients is Raleigh distributed; however, following previous work on indoor models, the IEEE 802.15.3c channel model uses log-normal distribution based on measurements at 60 GHz [11]. The measurement results also show that clusters can be assumed to fade independently from rays at 60 GHz. This requires a modification to (1.3), which can be written as

$$\alpha_{k,l} = p_{k,l}\xi_l\beta_{k,l} \tag{1.4}$$

where ξ_l and $\beta_{k,l}$ correspond to the fading associated with clusters and rays, respectively.

The log-normal distribution can be expressed as

$$20\log_{10}(\xi_l\beta_{k,l}) \propto \mathcal{N}(\mu_{k,l}, \sigma_1^2 + \sigma_2^2) \tag{1.5}$$

where

$$\mu_{k,l} = \frac{10\left[\ln(\Omega_0) - T_l/\Lambda - \tau_{k,l}/\lambda\right]}{\ln(10)} - \frac{(\sigma_1^2 + \sigma_2^2)\ln(10)}{20}. \tag{1.6}$$

In order to study the performance of networks with directional antennas, the IEEE 802.15.3c Task Group extended this model in (1.1) to include the DoA parameters. This has great importance since directional communications will be a very crucial part of 60 GHz networks. Several measurement campaigns indicated that rays arrive in clusters not only in time, but also in direction of arrival. Hence, the model in (1.1) is modified to include the DoA information as

$$h(t,\phi) = \sum_{l=0}^{L-1}\sum_{k=0}^{K_l-1} \alpha_{k,l}\delta(t - T_l - \tau_{k,l})\delta(\phi - \Theta_l - \theta_{k,l}) \tag{1.7}$$

where Θ_l is the mean angle of arrival of the lth cluster and $\theta_{k,l}$ is the angle of arrival of the kth ray from the lth cluster. Similar to the previous case, $\Theta_0 = 0$. The density of $\theta_{k,l}$ is expressed as

$$p(\theta_{k,l}) = K\exp(f(\theta_{k,l})) \tag{1.8}$$

where K is a normalization factor and function $f(\cdot)$ depends on the scenario [55]:

$$f(\theta_{k,l}) = -\left(\frac{\theta_{k,l}}{\sqrt{2}\sigma_G}\right), \text{where } \sigma_G \text{ is the standard deviation of the Gaussian distribution} \tag{1.9a}$$

$$f(\theta_{k,l}) = \kappa \cos\theta_{k,l}, \text{where } \kappa \geq 0 \text{ is the degree of non-isotropy of the Von-Mises distribution} \tag{1.9b}$$

$$f(\theta_{k,l}) = -\left(\frac{\sqrt{2}|\theta_{k,l}|}{\sigma_L}\right), \text{where } \sigma_L \text{ is the standard deviation of the Laplacian distribution.} \tag{1.9c}$$

All these functions can be characterized by the standard deviation σ_θ of the distribution (1.8), which is related to σ_G, σ_L or κ. The parameters of this model are extracted based on the procedures described in [12, 13].

1.3 Scope of the Thesis

The goal of this thesis is to develop novel and practical schemes to reduce multipath density in the 60 GHz wireless networks. It is well known that multipath effects cause inter-symbol interference (ISI) for high-speed signaling and ultimately limit the achievable data rate at any frequency band. It has been discussed previously that the spatial and temporal properties of the 60 GHz channel are quite different from those of the lower frequency bands; this leads to the need of new approaches to mitigate multipath effects in the 60 GHz band. Two main areas will be investigated in this thesis to mitigate the effects of multipath: a proper choice

of polarization for specific propagation conditions and directional communications in 60 GHz spectrum. Each of these approaches have been analyzed in detail, new algorithms have been proposed and respective performance changes in comparison to the proposed standard by IEEE have been observed.

1.3.1 Polarization Selection

Utilizing proper polarization type is one method to reduce the channel delay spread and ISI by limiting the multipath effects seen at the receiver. In Chapter 2, we will show that a proper choice of polarization for a specific propagation condition increases the performance by reducing the number of multipaths in 60 GHz wireless channels. It has been discussed in [4] that in comparison to scattering and diffraction, the influence of reflection dominates wave-boundary interactions in 60 GHz. Therefore, modification of reflection characteristics has direct effect on the properties of multipaths. The easiest way to change the characteristics of reflection is changing polarization of the wave.

It has also been shown that the orientation of the circular polarization may switch after each reflection. This phenomenon, combined with the fact that the cross oriented waves are rejected at the receiver antenna, makes the circular polarization a better candidate for line-of-sight (LOS) scenarios in the 60 GHz wireless channel. On the other hand, in non-LOS (NLOS) scenarios, due to the poor ability of 60 GHz waves to penetrate through obstacles, communication needs to rely on reflective paths. This requires the use of linear polarization for optimal perfor-

mance.

In Chapter 2, we will propose a modified channel model based on the IEEE 802.15.3c channel model that includes the effects of polarization. This proposed channel model provides a more general approach to utilize the 60 GHz channel compared to IEEE's channel model when omnidirectional antennas are used.

However, in order for this scheme to work efficiently, it is of utmost importance to know if the channel is LOS or NLOS to select an appropriate polarization scheme before transmitting data in 60 GHz wireless channel. In order to address this issue, in Chapter 2, we propose an algorithm to detect the network topology, i.e., if the channel is LOS or NLOS, without using any external information source (GPS, optical sensors etc.).

1.3.2 Directional Communication

When equipped with directional antennas, the steering of the transmitter and the receiver plays an important role in the performance of the wireless channel. In the case of a misalignment between the two ends of the channel, the received power could be severely reduced, which increases the error rate dramatically. Therefore, finding the correct transmission direction is critical when using directional antennas.

Direction finding is a complex process when location information of nodes in the network is not available *a priori*. This increased complexity is the only drawback that is introduced by the use of directional antennas when compared with

omnidirectional antennas. In Chapter 4, we will tackle this problem and show that the increase in complexity will be compensated with the increase of performance due to the efficient selection of transmission direction even without considering the increased gain of the antenna. Due to the unique characteristics of the 60 GHz propagation, the most efficient transmission direction is not necessarily the direct path between the transmitter and the receiver. In the LOS scenarios, the direct path is indeed the most efficient direction for transmission. On the other hand, in NLOS scenarios, when there is an obstruction on the direct path between the transmitter and the receiver, the most efficient direction for transmission will be one of the reflected paths since the penetration ability of electromagnetic waves is quite poor in the 60 GHz spectrum.

In Chapter 5, we will arange this direction detection algorithm in a network environment with changing number of nodes. We assume random events that might trigger the execution of this algorithm and observe the trade-off between the time consumed by the execution of direction detection algorithm and the performance increase due to the utilization of it.

Finally, in Chapter 6, we propose a double directional channel model for 60 GHz networks, which considers directional antennas for both the transmitter and the receiver and polarization effects. This proposed channel model is the most general channel model that has been created so far for a 60 GHz channel in the literature as of the writing of this thesis.

Bibliography

[1] P. F. M. Smulders, "Exploiting the 60 GHz band for local wireless multimedia access: prospects and future directions," *IEEE Commun. Mag.*, vol. 40, pp. 140–147, Jan. 2002.

[2] F. Giannetti, M. Luise, and R. Reggiannini, "Mobile and personal communications in 60 GHz band: A survey," *Wirelesss Personal Comunications*, vol. 10, pp. 207–243, 1999.

[3] R. C. Daniels and R. W. Heath, Jr., "60 GHz Wireless Communications: Emerging Requirements and Design Recommendations," *IEEE Vehicular Technology Magazine*, vol. 2, no. 3, pp. 41-50, Sep. 2007.

[4] P. Smulders, "Broadband wireless LANs: a feasibility study" PhD Thesis, Eindhoven Univeristy of Technology, The Netherlands, ISBN 90-386-0100-X, 1995.

[5] P. F. M. Smulders and A. G. Wagemans, "Wideband Indoor Radio Propagation Measurements at 58 GHz," *IEE Elect. Lett.*, vol. 28, no. 13, pp. 1270–1271, 1992.

[6] P. F. M. Smulders and G. J. A. P. Vervuurt, "Influence of Antenna Radiation Patterns on Mm-wave Indoor Radio Channels," Intl. Conf. Univ., Pers. Commun., Ottawa, Canada, pp. 631–635, Oct. 1993.

[7] S. Yong, "TG3c channel modeling sub-committee final report," *IEEE 802.15-07-0584-00-003c*, Jan. 2007 (https://mentor.ieee.org/802.15/file/07/15-07-0584-01-003c-tg3c-channel-modeling-sub-committee-final-report.doc).

[8] IEEE. Std. 802.15.3-2003 ed. Wireless Medium Access Control (MAC) and Physical Layer (PHY) Specifications for High Rate Wireless Personal Area Networks (WPANs).

[9] A. Sadri, "802.15.3c Usage Model Document (UMD), Draft," 15-05- 0055-21-003c, Jan. 2007 (ftp://ieee:wireless@ftp.802wirelessworld.com/15/06/15-06-0055-21-003c-mmwave-802-15-3c-usage-model-document.doc)

[10] A. Saleh and R. Valenzuela, "A statistical model for indoor multipath propagation," *IEEE J. Select. Areas Commun.*, vol. 5, no. 2, pp. 128–137, Feb. 1987.

[11] J. Foerster, "Path loss proposed text and S-V model information." IEEE P802.15-02380r0-SG3a, Jun. 2002.

[12] A. F. Molisch, U. G. Schuster, and C. C. Chong, "Measurement procedure and methods on channel parameter extraction." IEEE 15-04-283-00-4a, May 2004

[13] K. Balakrishnan *et al.*, "Characterization of ultra wideband channels: small-scale parameters for indoor & outdoor office environments." IEEE 802.15-04-0342-00-004a, July 2004.

Polarization Effects for Indoor Wireless Communications at 60 GHz

Ferhat Yildirim, Ali S. Sadri, and Huaping Liu

IEEE Communications Letters

September 2008

2.1 Abstract

This letter studies the performance of indoor wireless communication systems operating at 60 GHz with different polarization schemes. Circular polarization is known to reduce multipath effects in line-of-sight (LOS) environments in the 60 GHz band. We propose a modified channel model based on the IEEE 802.15.3c channel model to incorporate the polarization effects. We then use this model to evaluate the error performance of a wireless communication system that uses circular polarization. The results are compared with linear polarization for LOS environments.

2.2 Introduction

The 60 GHz unlicensed spectrum (57−64 GHz) is attractive for high-speed wireless personal area networks in indoor environments. It is well known that multipath effects cause intersymbol interference (ISI) for high-speed signaling and ultimately limit the achievable data rate at any frequency band. The spatial and temporal properties of the 60 GHz channel are quite different than those of the lower frequency bands [1,2]; this leads to the need of novel approaches to mitigate multipath effects in the 60 GHz band. Several approaches have been proposed to improve the performance of the 60 GHz wireless systems through phase noise suppression and different modulation techniques [2–4]. Use of directional antennas is also an effective method to mitigate multipath effects for the 60 GHz band [5–7].

In this letter, we study the possibility of using different polarizations to al-

leviate the multipath effect at 60 GHz. We modify the IEEE 802.15.3c channel model to incorporate the effect of circular polarization and numerically evaluate the improvement of using circular polarization in line-of-sight (LOS) propagation environments.

2.3 Channel Model with Circular Polarization

2.3.1 Circular polarization

In LOS communication environments, reflected, diffracted, and scattered waves from the nearby objects (i.e., indirect paths) cause multipath fading effects. It has been found based on the measurements in [8] that reflection is the dominating factor affecting the channel delay at 60 GHz, whereas the significance of diffraction and penetration decreases as frequency increases. Hence, at 60 GHz, one can control the channel delay by changing the reflection characteristics of the wave, which depends on the reflecting material and the incident wave (polarization and the incident angle) [9]. Since channel delay relative to the bit interval determines the level of ISI, the reflection characteristic of waves has a direct influence on the error performance of the wireless communication systems at 60 GHz. The simplest way to change the reflection characteristics of a wave is to change its polarization.

The reflection characteristic of circularly polarized waves is quite different from that of linearly polarized waves. For certain incident angles the handiness of a circularly polarized wave switches upon reflection [10]. Theoretically, a circular

polarized antenna rejects a cross polarized incoming wave; however, in practice, the received wave would experience a finite attenuation (e.g., 20 dB). Even with this finite attenuation, appropriately use of polarization could lead to significantly reduced channel delay spread, and hence improved error performance for high-rate communications.

2.3.2 Impulse response model

Several channel models (e.g., [11–14]) and measurement results (e.g., [15, 16]) can be found in the literature along with our more recent measurement results [17] for the 60 GHz band. In this letter, we use a similar channel model that is developed by the IEEE 802.15.3c Task Group [12], which models both time and angle of arrival statistics of the received rays. We use a time-dependent variation of this model to compare the effects of polarization on the system performance. The channel impulse response of this model is expressed as

$$h(t) = a_{\text{LOS}}\delta(0) + \sum_{l=0}^{L-1}\sum_{k=0}^{K-1} a_{l,k}\delta(t - T_l - \tau_{l,k}) \tag{2.1}$$

where T_l and $\tau_{l,k}$ are the arrival times for clusters and rays within a cluster, respectively, a_{LOS} is the coefficient for the direct path, and $a_{l,k}$ is the coefficient of the k-th ray of the l-th cluster.

Several scenarios have been proposed in [12]. In this letter, we focus on indoor LOS models CM1, CM5, and CM10 for residential room, library, and hallway

scenarios, respectively. For practical systems that operate at high data rates in the 60 GHz band, the deployment is most likely required to have an LOS component between the transmitter and the receiver. Thus, these environments represent a useful scenario that is likely to be encountered in practice. We assume that both the transmitter and receiver are equipped with an omnidirectional antenna.

Although deployment of most of the 60 GHz networks is for LOS environments, NLOS scenarios cannot be avoided. In NLOS environments, due to the high penetration loss of 60 GHz signals through objects, reflected paths must be relied on for effective communications. In such a case, directive antennas could increase the system performance by focusing the radiated power in a certain direction. However, networks with directional antennas require more sophisticated medium access control (MAC) algorithms. Issues with 60 GHz networks using directional antennas along with a proposed directional MAC algorithm are discussed in [18].

2.3.3 Incorporation of polarization

The model proposed by the IEEE 802.15.3c Task Group [12] is based on linear polarization. Thus, we need to modify the model given in (2.1) to incorporate the effects of circular polarization.

In multipath environments, each path may experience multiple reflections before it reaches the receiver. Let m represent the order-of-arrival (OoA) of paths. The incident angle of each reflection, θ_i, is an independent and identically distributed random variable. We define a threshold angle, θ_T, for which the handiness

of the circular polarization switches after reflection when $\theta_i \leq \theta_T$. The value of θ_T depends on the material properties of the reflective surface. The probability of handiness being switched after a reflection can be written as $p_s = F_{\theta_i}(\theta_T)$, where $F(\cdot)$ is the cumulative distribution function of θ_i.

Let p_a represent the probability that a path experiences odd number of handiness switching from the transmitter to the receiver. Such a path will be significantly attenuated (or eliminated in the ideal case) due to cross-pol suppression. In order to incorporate the effect of circular polarization into the channel model (2.1), we need to establish the relationship between p_a, which depends on p_s, and m. Note that for the LOS path ($m = 0$), $p_a = 0$.

For simplicity, let us consider the first 50 multipath components. This is sufficient for most practical applications since paths arrived after this large index would be too weak to have a non-negligible impact on the system performance. From extensive ray tracing simulation results, we observe that the statistical behavior of early-arrival paths ($m \leq 11$) is different than that of later-arrival ones ($m > 11$). For all channel model scenarios considered (library, hallway, and residential room), it is observed that the paths with $m \leq 11$ (excluding the LOS component) arrive at the receiver via either one or two reflections with a probability equal to 1. Therefore, for the OoA index region $m = (0, 11]$, the probability that a path will experience a significant cross-pol attenuation is expressed as

$$p_a = \lambda(m)p_s + 2(1 - \lambda(m))p_s(1 - p_s) \tag{2.2}$$

where $\lambda(m)$ is the probability of a path having only one reflection. Ray tracing simulations also show that the first two multipaths from the transmitter to the receiver have only one reflection with a probability 1 for all channel model scenarios. Hence, for $m = 1$ and 2, $\lambda(m) = 1$ and $p_a = p_s$.

The function $\lambda(m)$ is derived using the ray tracing simulation for all channel model scenarios. The distribution of $\lambda(m)$ along with the model created to approximate these distributions is shown in Fig. 2.1. Since $\lambda(m)$ versus m for the three channel environments considered are similar, we use a single model to represent $\lambda(m)$. This model is written as

$$\lambda(m) = \begin{cases} 1, & 1 \leq m \leq 2 \\ am^4 + bm^3 + cm^2 + dm + e, & 3 \leq m \leq 11 \end{cases} \tag{2.3}$$

where $a = -0.001$, $b = 0.0289$, $c = -0.2488$, $d = 0.6251$, and $e = 0.5788$.

For the later-arrival paths ($m > 11$), the probability that they arrive at the receiver with an odd number of handiness-switched reflections is equal to $p_a = 0.5$. Therefore, for any m, the probability that a path will experience a significant cross-pol attenuation can be written as

$$p_a(m) = \begin{cases} 2p_s^2(\lambda(m)-1) - p_s(\lambda(m)-2), & 1 \leq m \leq 11 \\ 0.5, & m \geq 12. \end{cases} \tag{2.4}$$

We use the information obtained from (2.4) to modify the channel model (2.1)

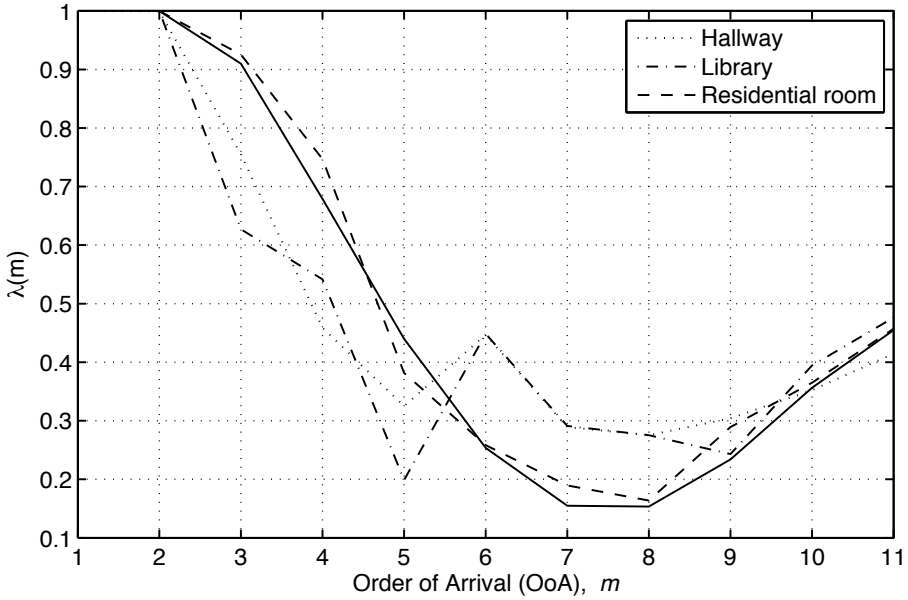

Figure 2.1: The probability of each ray experiencing a single reflection before reaching the receiver for OoA index $m \leq 11$.

by creating a binary array of length 51 as

$$\boldsymbol{q} = [q_0 \; q_1 \; \cdots \; q_{50}] \tag{2.5}$$

where q_m takes on the values of A or 1 with probabilities $p_a(m)$ and $1 - p_a(m)$, respectively. The quantity A is the additional attenuation that the m-th ray experiences due to the cross-pol rejection of circular polarization. The special case of $A = 0$ corresponds to the theoretical case of infinite attenuation; a finite number corresponds to the more realistic cross-pol rejection (typically 15-20 dB). The value of q_0, which corresponds to the direct path, is always equal to 1.

We can thus modify the channel model in (2.1) to incorporate the effect of

circular polarization as

$$h(t) = a_{\text{LOS}} q_0 \delta(0) + \sum_{l=0}^{L-1} \sum_{k=0}^{K-1} a_{l,k} q_m \delta(t - T_l - \tau_{l,k}). \tag{2.6}$$

The value of m is related to k and l in a complex manner that depends T_l and $\tau_{l,k}$. Instead of dealing with this complex relation, we take a statistical approach for analysis and simulation. In this approach, we obtain the delay and fading coefficients of the paths using model (2.1), and then apply the modification vector given in (2.5).

Clearly, circular polarization will not work well in NLOS environments since the dominant reflected path must be exploited, rather than be suppressed with a non-zero probability. Also note that the special case with $q_m = 1,\ \forall m$, of the modified model (2.6) is simply the channel model for linear polarization.

2.4 Simulation

We simulate the bit-error rate (BER) performance of a system that employs pulse-shaped binary phase-shift keying (BPSK) modulation and operates at a rate of 500 Mbps. The major parameters and values of the channel models are summarized in Table 2.1; more related parameters can be found in [12]. We consider concrete as the reflective medium and the cross-pol rejection for receiver antennas is 20 dB for all propagation scenarios. The threshold of the incident angle is chosen to be $\theta_T = 50$ such that 10% or less power of the incident wave is reflected back with

Table 2.1: Channel Parameters used in Simulation

Parameter	Residential	Library	Hallway
Path loss exponent	1.53	3	2.29
Free space path loss intercept (dB)	75.1	50	69.7
Cluster arrival rate (1/ns)	1/4.76	0.25	1
Ray arrival rate (1/ns)	1/1.30	4	1
Cluster decay factor	4.19	12	1
Ray decay factor	1.07	7	7
Mean number of clusters	4	17	1
Handiness switching probability, p_s	0.45	0.24	0.26

the same handiness. We obtain the probability distribution of θ_i from ray tracing, which considers 10^{10} different reflections for each application scenario. The values of p_s in Table 2.1 are obtained by $p_s = F_{\theta_i}(\theta_T)$, where $F_{\theta_i}(\cdot)$ was defined at the beginning of Section 2.3.3.

Some common blocks of a wireless communication system such as channel coding and interleaving are not included so that we can clearly assess the impact of polarization on error rates of the raw data bits.

Fig. 2.2 shows the BER performance of the BPSK system in different LOS environments. For all scenarios, it is observed that circular polarization performs better than linear polarization in reducing the raw bit-error rates. The residential environment retains limited number of multipaths, with a delay spread of 0.1-0.2 ns; hence, the performance improvement due to circular polarization is insignificant. On the other hand, the library and hallway environments are severely affected by reflected paths and have a delay spread of a few ns. For these cases,

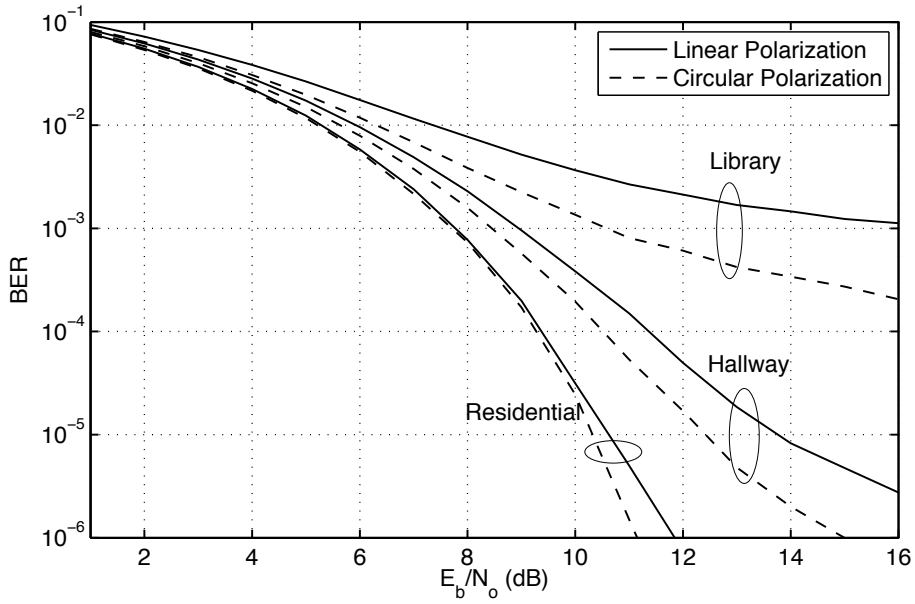

Figure 2.2: BER performance of a BPSK system with linear and circular polarizations in various LOS environments. Square-root raised cosine filter is used with a roll-off factor of 0.3. 2000 blocks are simulated with a block length of 200 and 20 samples per symbol.

the improvement in error performance due to the use of circular polarization in LOS environments is substantial, as clearly observed in Fig. 2.2.

2.5 Conclusion

We have explored the error performance of 60 GHz wireless communications using different antenna polarizations. We first extended the channel impulse response model developed for 60 GHz wireless communications with linear polarization to incorporate the effects of circular polarization. The statistics used in the extended model are obtained by ray-tracing simulation. Using the extended model, we then

simulated the error performance of a coherent BPSK system with linear and circular polarizations in LOS environments. We found that in LOS environments, circular polarization reduces the multipath effect, and thus provides better performance than linear polarization approach, especially for systems operating at high data rates.

Bibliography

[1] H. Xu, V. Kukshya and T. Rappaport, "Spatial and temporal characteristics of 60-GHz indoor channels," *IEEE J. Select. Areas Commun.*, vol. 20, no. 3, pp. 620–630, Apr. 2002.

[2] A. Bourdoux, J. Nsenga, W. Van Thillo, F. Horlin and L. Van der Perre, "Air interface and physical layer techniques for 60 GHz WPANs," in *Proc. Int. Symp. on Comm. and Veh. Tech.*, Nov. 2006, pp. 1–6.

[3] H. Kim, K. Ahn and H. Baik, "Phase noise suppression algorithm for OFDM-based 60 GHz WLANs," in *Proc. Int. ISWPC*, Jan. 2006, pp. 4.

[4] T. Chen, H. Zhang and I. Chlamtac, "High speed orthogonal waveform based indoor wireless transmission by an UWB and 60 GHz dual band system," in *Proc. ISWCS'06*, Sep. 2006, pp. 423–427.

[5] H. El Ghannudi, L. Clavier, A. Bendjaballah, A. Boe and P. Rolland, "Performance of IR-UWB at 60 GHz for ad hoc networks with directive antennas," in *Proc. IEEE ICUWB'06*, Sep. 2006, pp. 149–154.

[6] S. Pinel, I. Kim, K. Yang and J. Laskar, "60 GHz linearly and circularly polarized antenna arrays on liquid crystal polymer substrate.," in *Proc. Euro. Microwave Conf.*, Sep. 2006, pp. 858–861.

[7] S. Lei, S. Houjun, L. Deng and C. Yong, "Study of the improved mm-wave omni-directional microstrip antenna," in *Proc. ISAPE'06*, Oct. 2006, pp. 1–4.

[8] P. Smulders, "Broadband wireless LANs: a feasibility study" Ph.D. Thesis, Eindhoven Univversity of Technology, The Netherlands, ISBN 90-386-0100-X, 1995.

[9] B. Langen, G. Lober and W. Herzig, "Reflection and transmission behaviour of building materials at 60 GHz," in *Proc. IEEE PIMRC'94*, vol. 2, Sep. 1994, pp. 505–509.

[10] K. Sato, *et al.* "Measurement of reflection and transmission characteristics of interior structures of office building in the 60-Ghz band," *IEEE Trans. Antennas Propagat.*, vol. 45, pp. 1783–1791, Dec. 1997.

[11] N. Moraitis and P. Constantinou, "Measurements and characterization of wideband indoor radio channel at 60 GHz," *IEEE Trans. Wireless Commun.*, vol. 5, no. 4, pp. 880–889, Apr. 2006.

[12] S. Yong, "TG3c channel modeling sub-committee final report," *IEEE 802.15-07-0584-00-003c*, Jan. 2007 (https://mentor.ieee.org/802.15/file/07/15-07-0584-01-003c-tg3c-channel-modeling-sub-committee-final-report.doc).

[13] J. Hubner, S. Zeisberg, K. Koora, J. Borowski and A. Finger, "Simple channel model for 60 GHz indoor wireless LAN design based on complex wideband measurements," in *Proc. IEEE VTC'97*, vol. 2, May 1997, pp. 1004–1008.

[14] T. Zwick, T. Beukema and H. Nam, "Wideband channel sounder with measurements and model for the 60 GHz indoor radio channel," *IEEE Trans. Veh. Technol.*, vol. 54, no. 4, pp. 1266–1277, Jul. 2005.

[15] D. Matic, H. Harada and R. Prasad, "Indoor and outdoor frequency measurements for MM-waves in the range of 60 GHz," in *Proc. IEEE VTC'98*, vol. 1, May 1998, pp. 567–57.

[16] J. Kunisch, E. Zollinger, J. Pamp and A. Winkelmann, "MEDIAN 60 GHz wideband indoor radio channel measurements and model," in *Proc. IEEE VTC'99*, vol. 4, Sep. 1999, pp. 2393–2397.

[17] A. Sadri, A. Maltsev, and A. Davydov, "IMST time-angular characteristics analysis," *IEEE 802.15-06-0141-00-003c*, Mar. 2006 (https://mentor.ieee.org/802.15/file/06/15-06-0141-01-003c-imst-time-angular-characteristics-analysis.ppt).

[18] F. Yildirim and H. Liu, "Directional MAC for 60 GHz using polarization diversity extension (DMAC-PDX), *in Proc. IEEE Globecom07*, Nov. 2007.

Incorporation of Appropriate Polarization Selection into the 60 GHz Wireless Networks

Ferhat Yildirim and Huaping Liu

3.1 Abstract

Due to the unique characteristics of electromagnetic waves at 60 GHz, polarization can be effectively used to decrease the number of multipaths in 60 GHz channel, which increases the inter-symbol interference of the wireless system. In this paper, we propose a practical implementation of proper polarization selection for 60 GHz channel, which detects the topology of the network, i.e., LOS or NLOS, without using any prior knowledge. It has been shown that the complexity introduced by the proposed algorithm is not only compensated by the increase in efficiency, but also the overall performance increased.

3.2 Introduction

The increasing demand for high-speed wireless networks in recent years and exhaustion of spectrum resources have motivated the use of the higher frequency region of the radio spectrum. The 60 GHz band has recently been explored for high-speed, short-range wireless network applications [1–3]. Similar to lower frequency bands, 60 GHz channel also suffers from inter-symbol interference (ISI) created due to excessive multipaths in indoor environments. However, there are many challenges while porting solutions that are designed for the lower frequency band wireless networks to 60 GHz spectrum due to the unique characteristics of 60 GHz radio frequency (RF) signals. These unique features include the inability of signal penetration through obstacles [4], high free-space path loss [5],and absorption of signal energy by gases like oxygen molecules, water vapor, and hydrometeors

in the form of rain or snow [6].

Utilizing proper polarization type is one method to reduce the channel delay spread and ISI by limiting the multipath affect seen at the receiver. In our previous work, [7], we showed that proper selection of polarization increases the performance by reducing the number of multipaths in 60 GHz wireless channel. In [7], we concluded that for LOS scenarios, use of circular polarization increases the probability of multipath rejection at the receiver antenna level, which in turn reduces the ISI and bit-error-rate of the system. On the other hand, however, in non-LOS (NLOS) scenarios, due to the inability of waves to penetrate through obstacles, communication needs to rely on reflective paths and linear polarization for optimal performance.

In the light of the conclusion of [7], it is utmost important to know if the channel is LOS or NLOS to select an appropriate polarization scheme before transmitting data in the 60 GHz wireless channel. In this paper, we propose an algorithm to detect the network topology, i.e., if the channel is LOS or NLOS, without using any external information source (GPS, optical sensors etc.). This algorithm relies on the unique characteristics of electromagnetic waves at 60 GHz band. We assume a dynamic channel, where nodes are mobile, hence the topology is changing over time. We analyze the proposed algorithm in a network scenario and show that, the complexity introduced by utilizing the proposed algorithm is compensated by the performance gained by the use of proper polarization selection.

3.3 Polarization Selection in 60 GHz Networks

In wireless communications, reflected, diffracted, and scattered waves from the nearby objects cause multipath fading effect, which degrades the system performance. In comparison with the other wave-medium boundary interactions, reflection is the dominating factor that effects the channel delay at 60 GHz [8]. The significance of diffraction and penetration decreases as frequency increases. This has been illustrated in Fig. 3.1 for a typical office environment using ray-tracing method [9]. It is clearly observed that the inclusion or exclusion of penetration and diffraction does not affect the rms delay spread at 60 GHz. Hence, one can only control the channel delay by changing the reflection characteristics of the wave. Since channel delay relative to the bit interval determines the level of ISI, we can conclude that reflection characteristics of waves has a direct influence on the error performance of the wireless communication system at 60 GHz. One way to change the reflection characteristics of a wave is to change its polarization.

Polarization of an electromagnetic wave is the trace of the electric field vector on the plane that is perpendicular to the direction of propagation. If the ratio of the magnitude of the two orthogonal components of the electric field vector is constant and there is no phase difference between these components, the wave is linearly polarized. Two special cases for linear polarization are vertical and horizontal polarizations. When the two orthogonal components have the same magnitude but a 90 degree phase difference, the wave is circularly polarized. Depending on the leading orthogonal component in phase, i.e., direction of rotation, circular polar-

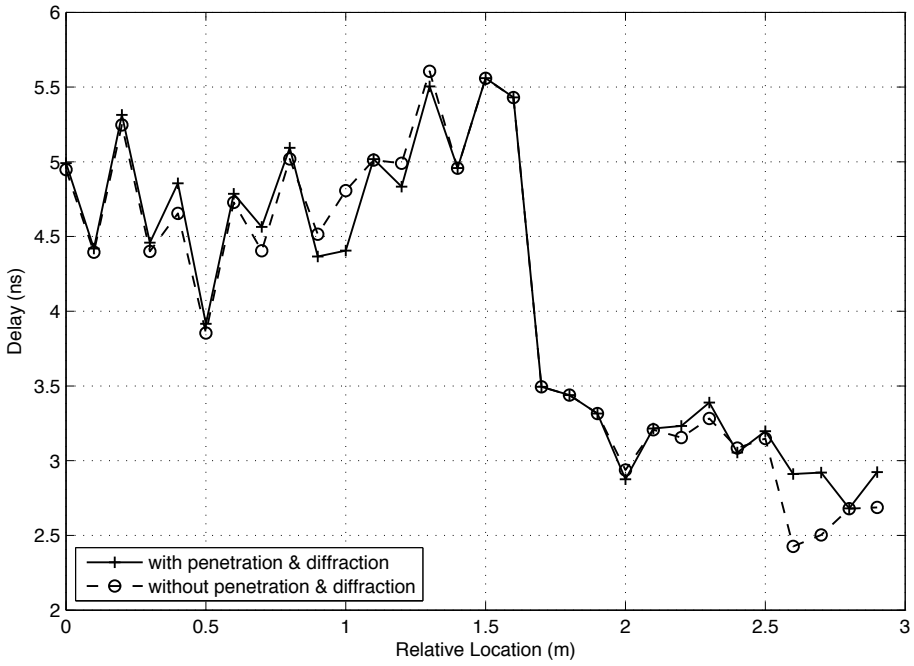

Figure 3.1: Delay spread for a receiver line at 60 GHz. A typical office environment is simulated with a dimension of 5×7 meters and a height of 3.5 meters; it is filled with typical office furniture and couple of people that will create some shadowing effects. The transmitter is placed one meter above the ground level. We compare the delay spread with and without the effects of diffraction and penetration.

ization is classified into two subclasses: right-hand circular polarization (RHCP) and left-hand circular polarization (LHCP) [10].

The reflection characteristics of circularly polarized waves are quite different from that of linear polarized waves [11]. For certain incident angles the handiness of a circularly polarized wave switches upon reflection [12]. Theoretically, a RHCP antenna will completely reject LHCP waves, and vice versa. If the incoming wave is linearly polarized, a RHCP antenna introduces an additional attenuation of 3 dB. This rejection or attenuation requires no further processing as it occurs at the

physical antenna layer [10]. However, in practice, the cross-polarization rejection is finite and varies between 10-20 dB [13]. Even with this finite attenuation, appropriately use of polarization could lead to significantly reduced channel delay spread, and hence improved error performance for high-rate communications.

In our previous study [7], we have statistically derived the probability of orientation switching for each reflection and proposed a channel model that includes the effects of polarization in 60 GHz wireless networks. Using simulation, we have showed that, in LOS scenarios, use of circular polarization increases the probability of multipath rejection at the receiver antenna level, which in turn reduces the ISI and increases the error performance of the system. On the other hand, however, in NLOS scenarios, due to the inability of waves to penetrate through obstacles, communication needs to rely on reflective paths, which requires the use of linear polarization for optimal performance.

3.4 Network Topology Detection

Two key issues must be solved in order to exploit the advantage of proper polarization selection that has been summarized in the previous section: (a) how to determine if the channel is LOS (i.e., direct path is present) or NLOS (i.e., direct path is absent) without invoking complex algorithms, and (b) how to switch polarization in a dynamically changing environment.

The second issue can be solved by using a dual polarized smart antenna at the transmitter side [14]. The first issue mentioned above can be effectively solved by

exploiting the different reactions of linear and circular polarization to multipath propagation as discussed in [7]. Using a dual polarized antenna, a test frame (TEST) is sent in an omnidirectional fashion with linear and circular polarizations simultaneously with transmit power

$$P_T = P_{T,l} = P_{T,c}, \tag{3.1}$$

where $P_{T,l}$ and $P_{T,c}$ are transmit power for linear and circular polarized TEST frames, respectively. In order to avoid interference, these transmissions may occupy different time slots or different frequency bands. However, this multiple access scheme needs to assure that the channel is as similar as possible for both TEST frames. On the other end of the channel, the receiver is also equipped with a dual polarized antenna, which can detect both linear and circular polarized waves; however, the handiness of the circular polarized antenna is inverted with respect to the transmitter antenna in the detection stage. Under this setup, the power of the first received path with linear and circular polarized receive antennas can be written as

$$P_{R,l} = P_{T,l} - P_L - P_{\text{ref}}, \tag{3.2a}$$

$$P_{R,c} = P_{T,c} - P_L - P_{\text{ref}} - K_{\text{co}}. \tag{3.2b}$$

where P_L is the propagation path loss, P_{ref} is the loss due to possible reflections, and K_{co} is the cross polarization rejection ratio of the antenna that applies to the

co-polarized waves (same handiness) with respect to transmitter antenna.

In LOS scenarios, it is expected that, the first arrival path is the direct path, hence $P_{\text{ref}} = 0$. Note that K_{co} is typically around 20 dB. Even with a finite K_{co}, $P_{R,c}$ is significantly attenuated due to cross handiness, and the power difference between the two frames,

$$\delta_R = P_{R,l} - P_{R,c}, \tag{3.3}$$

can be calculated. Therefore, the classification of the communication environment can be easily made: if $\delta_R \leq K_{\text{co}}$, environment is LOS; otherwise, it is NLOS. In NLOS scenarios, although the reflection loses to the same path for linear and circular polarizations differ slightly, this difference is negligible when compared to K_{co}.

This algorithm differentiates LOS and NLOS by detecting the presence or absence of a reflection for the first arrival path using unique reflection characteristics of circular polarization and the lack of scattering and penetration in the 60 GHz channel. The result of this detection is reported back to the transmitter by sending either ACK/LOS or ACK/NLOS frames. Transmitter, upon receiving either of the ACK frames switches the antenna polarization accordingly; circular polarization for LOS, and linear polarization for NLOS. This algorithm is explained in detail in Appendix A.

3.5 Throughput Analysis

The proposed algorithm, which is detailed in the previous section, utilizes the unique features of electromagnetic waves at the 60 GHz spectrum to detect weather the wireless channel between the transmitter and receiver is LOS or NLOS. However, while doing this, it introduces some additional overhead to the physical (PHY) layer. In order for the proposed algorithm to work, TEST frames need to transmitted and an ACK frame need to be received. This additional transmission requires extra time. In this section, we analyze the throughput of such wireless system and show that the additional time required by the proposed algorithm is compensated by the increased error-performance due to proper selection of polarization.

The throughput of a system is calculated as the ratio of the successfully transmitted bits to the total transmission time [15]. Normalized throughput (S_n), on the other hand, is defined as the ratio of the throughput to the data rate, R_d. In an ideal error-free channel, a longer frame results in a higher throughput. However, for practical indoor wireless channels where both noise and ISI are present, a longer frame length does not necessarily result in higher throughput. This is because a single bit error in the frame might require the retransmission of that frame if no error correction algorithm is being employed; this decreases the throughput of the system significantly. Retransmission of erroneous frames is necessary for data transmission, e.g. link between external storage and computer, however is not required to some extend in streaming media, e.g. video transmission between source to display.

Table 3.1: Parameters of Throughput Analysis

Parameter	Value
Size of ACK, L_a	14 bytes
Size of TEST, L_t	14 bytes
Size of frame, L	to be optimized
Propagation delay, t_p	9.4ns
Channel listening delay, t_l	$\sim 2t_p$
Base rate, R_b	54 Mbps
Data rate, R_d	1Gbps

Parameters used in the derivation of the optimum throughput are listed in Table 3.1. The parameter values are selected for a typical 60 GHz indoor environment [16]. The base rate, R_b, is used for transmission of auxiliary frames such as ACK, TEST; the data rate, R_d, is used to transmit the payload. For a bit sequence of length x, the probability of successful transmission is

$$p_s = (1 - p_e)^x, \tag{3.4}$$

where p_e is the probability of bit error. We can write the bit-sequence length of the transmission for a single data frame, x, as

$$x = L + L_a + p_d(L_a + L_t), \tag{3.5}$$

where all parameters are defined in Table 3.1, and p_d is the probability of a required detection. If we assume the worst-case scenario, where the nodes are mobile and topology has to be recalculated before each data frame is sent, then $p_d = 1$.

Although this might not be common for deployment of 60 GHz indoor wireless networks, it is appropriate to consider the worst-case throughput to observe the efficiency of the proposed algorithm. Considering (3.5), the total time to transmit the data can be written as

$$t = \frac{L}{R_d} + 2t_p + 2t_l + p_d(\frac{L_a + L_t}{R_b}). \tag{3.6}$$

Using (3.4)-(3.6), the normalized throughput can be calculated as

$$S_n = (L/R_d)p_s/t. \tag{3.7}$$

It has been shown in [16] that

$$\lim_{L\to 0} S_n = 0 \tag{3.8a}$$

$$\lim_{L\to \infty} S_n = 0, \tag{3.8b}$$

and there exists an optimum data frame length, L_{opt}, for a given BER value. This is easy to understand for a non-ideal channel (i.e., one with a non-zero BER): as $L \to \infty$, it becomes impossible to transmit any successful data frame; as $L \to 0$, $S_n \to 0$ since no data are transmitted.

3.6 Communication Environment

The algorithm detailed in Section 3.4 is tailored for 60 GHz PHY, hence it is reasonable to assess its performance based on the scenarios that are defined by the IEEE 802.15 Task Group 3c, who proposed the standard for 60 GHz wireless communication. Among the five proposed usage models by IEEE 802.15 Task Group 3c, two of them are designated as mandatory. The usage models as defined in [17] are UM1, uncompressed video streaming from set-top box to HDTV, and UM5, data download from kiosk to handheld device, is designated as a mandatory usage model; UM2, multiple uncompressed video streaming; UM3, office desktop environment; and UM4, conference room ad-hoc network structure, are designated as optional usage models.

In addition to the usage models, several channel models for 60 GHz PHY are also proposed in the standard; some of which are associated with the usage models. The usage models and their associated channel models are listed in Table 3.6. All models assume indoor scenarios with relatively stationary nodes. The structure of the network is neither ad-hoc, nor infrastructure. Although any device can communicate with another one, the link can be established without any hops or intermediary nodes.

During the normal operation of a network, random events such as addition or removal of nodes, change of location and number of nearby scatterers (including users) and relocation of nodes could occur. Each of these events may change the distribution of the network in such a way that nodes need to re-detect the topology.

Table 3.2: Usage Models and Simulation Environments

UM1	Point to point video	Residential LOS
UM2	Point to multi-point video	Residential LOS and NLOS
UM3	Wireless desktop	Desktop LOS and NLOS
UM4	Conference	Office LOS
UM5	Kiosk	Hallway LOS

The re-detection probability, p_d that has been introduced in the previous section is related with the frequency of such events. One should note that, based on the usage models defined by the IEEE Task Group, we expect very low values for p_d as most models assume fairly stationary networks. However, we still study the extreme case of $p_d = 1$ to observe the performance of the proposed algorithm in the worst possible scenario. Moreover, in our analysis we assume that MAC layer would handle any packet collisions, channel access since these are beyond the scope of this paper. In this paper, we define and analyze the proposed algorithm strictly in the PHY layer.

3.7 Performance Analysis

We analyze the performance of the proposed algorithm using the throughput analysis of Section 3.5. We have selected three common environments that are defined in the IEEE 802.15.3c standard, namely residential, library and hallway scenarios. Although the error-performance analysis of these environments are used in the performance analysis of the proposed algorithm, they will not be repeated here due

to their appearance in [7]. Based on the error-performance analysis, we already know that circular polarization creates a very high error-rate in NLOS scenarios in such a way that it renders the wireless system practically inoperable. Therefore, we skip the NLOS analysis, as the proposed algorithm should always be used for best performance in NLOS situation.

For LOS case, on the other hand, the variation of normalized throughput with respect to data frame length in bytes is illustrated in Fig. 3.2. Note that, in each of the analyzed environment, use of linear polarization (which corresponds to not utilizing the polarization selection approach of [7]) in LOS scenario has lower throughput regardless of data frame length. The general difference between variation curves for each environment arises from the reflective behavior of the environment. Residential environment, for example, is defined with very small number of reflective surfaces in a large, mostly empty room. On the other hand, library environment is filled with shelfs and books and has significantly more multipaths compared to other environments. More multipaths in an environment, i.e., higher channel delay, yields to a lower throughput; however, the improvement due to the use of circular polarization is greater.

In Fig. 3.3 we present the normalized throughput with respect to the re-detection probability, p_d, which serves as the ultimate analysis for the efficiency of the proposed algorithm. We change p_d from zero (no re-detection) to one (re-detection before the transmission of each data frame) in a logarithmic scale. Considering the fact that the environments and usage models defined by IEEE 802.15.3c are mostly static networks, the re-detection is not something to happen

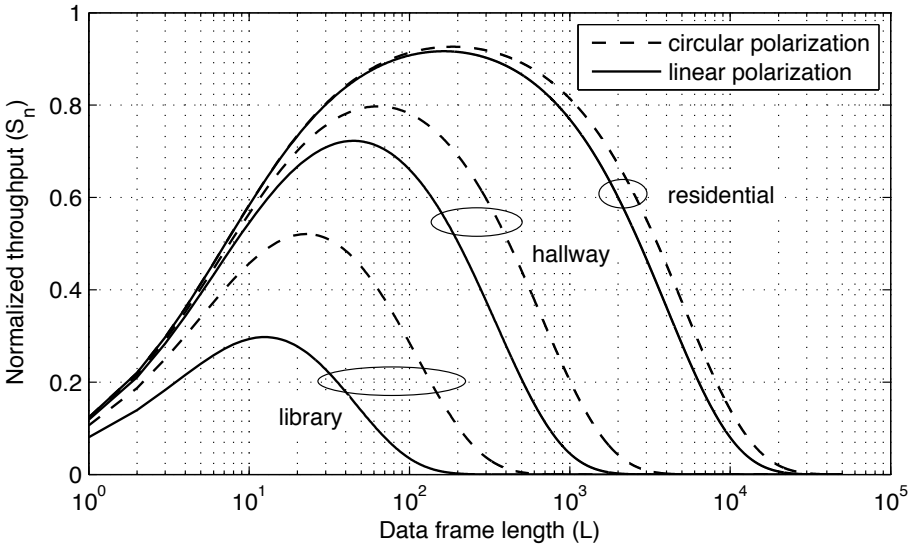

Figure 3.2: Data frame length distribution in bytes for different environments in 60 GHz channel, when $p_d = 0$. Optimum data frame length is 1488 bits, 512 bits and 184 bits for residential, hallway and library environments, respectively under circular polarization; 1312 bits, 360 bits and 104 bits for residential, hallway and library environments, respectively under linear polarization.

very frequently. For an average human walking speed of 1m/s, the corresponding re-detection probability is approximately 10^{-6}. Moreover, a $p_d = 10^{-5}$, corresponds to an approximate 10 events per second, which is considered as an extremely dynamic network in the context of 60 GHz indoor wireless systems, and a $p_d = 1$ value is an impractical situation and studied only for theoretical limit analysis.

The vertical dashed lines in Fig. 3.3 corresponds to the throughput value of the wireless system without the use of optimum polarization selection and the proposed algorithm for each environment. Once again it is easy to observe the effect of multipath density on the channel as residential environment has very little improvement, when compared to the library environment. However, the

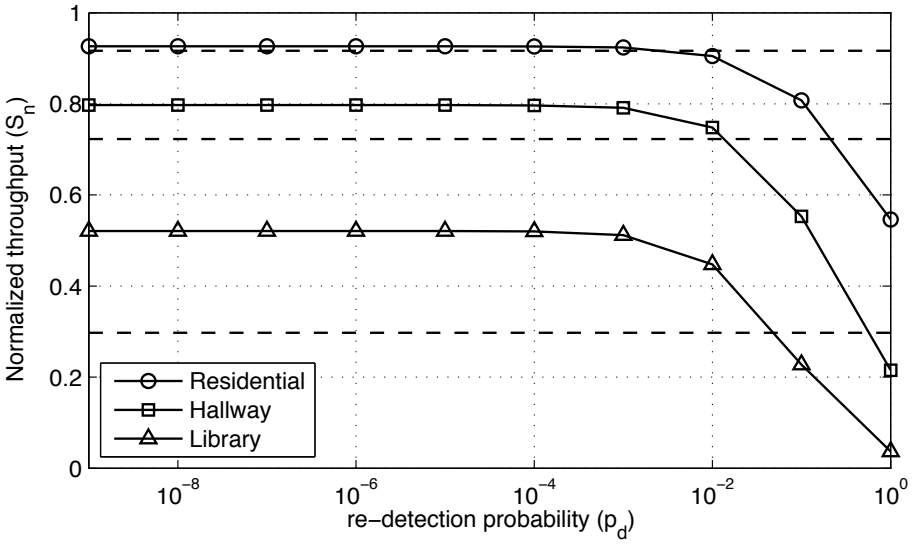

Figure 3.3: Normalized throughput with respect to re-detection probability for three different environments in 60 GHz channel. The dashed lines corresponds to the normalized throughput value of each corresponding environment when optimum polarization selection and the proposed algorithm is not used. Note that, for a practical 60 GHz indoor wireless network, the re-detection probability is typically between 10^{-5} and 10^{-6}.

most important conclusion out of the analysis of Fig. 3.3 is the fact that within the limits of practicality, the use of optimum polarization selection and the proposed topology detection algorithm is better than not using it at all. The complexity introduced by the proposed topology detection algorithm is not only compensated by the increased efficiency due to the better use of polarization, but also the overall throughput is increased.

Looking at the Fig. 3.3 for all environments, the algorithm starts to be inefficient when the network exceeds 10^4–10^5 events per second threshold, which is highly impractical.

3.8 Conclusion

In this paper, we proposed a topology detection algorithm in order to detect the presence or the absence of a direct path between the transmitter and the receiver in the 60 GHz channel. Such information can be employed for proper selection of polarization, which is proven to increase the performance of the network for 60 GHz wireless indoor systems. Using the derived throughput analysis, we have shown that the complexity introduced by the proposed algorithm is compensated by the increased efficiency due to the proper selection of polarization within the practical usage limits of indoor wireless systems.

Bibliography

[1] Federal Communications Commission, "Amendment of parts 2, 15 and 97 of the commissions rules to permit use of radio frequencies above 40 GHz for few radio applications," *FCC 95-499*, ET Docket No. 94-124, RM- 8308, Dec. 15, 1995.

[2] P. F. M. Smulders, "Exploiting the 60 GHz band for local wireless multimedia access: prospects and future directions," *IEEE Commun. Mag.*, vol. 40, pp. 140–147, Jan. 2002.

[3] C. J. Gibbins, "Radiowave propagation in the 30-60 GHz band," *IEE Colloquium Radiocomm. in the Range 30-60 GHz*, pp. 1/1-1/4, Jan. 1991.

[4] C. Koh, "The benefits of 60 GHz unlicensed wireless communications," *YDI Wireless White Paper 041104A*, Nov. 2003.

[5] M. Marcus and B. Pattan, "Millimiter wave propagation: spectrum management implications," *IEEE Microwave Mag.*, pp. 54–62, Jun. 2005.

[6] A. J. Richardson and P. A. Watson, "Use of the 55–65 GHz oxygen absorption band for short-range broadband radio networks with minimal regulatory control," *IEE Proceedings*, vol. 137, no. 4, Aug. 1990.

[7] F. Yildirim, A. S. Sadri, and H. Liu, "Polarization effects for indoor wireless Communications at 60 GHz," *IEEE Commun. Lett.*, vol.12, no.9, pp.660-662, Sep. 2008.

[8] P. Smulders, "Broadband wireless LANs: a feasibility study" Ph.D. Thesis, Eindhoven University of Technology, The Netherlands, ISBN 90-386-0100-X, 1995.

[9] RadioPlan RPS simulator, http://www.rps.com

[10] C. A. Balanis, *Advanced engineering electromagnetics*. New York: Wiley, 1989.

[11] I. Katz, "Radar reflectivity of the ocean surface for circular polarization," *IEEE Trans. Antennas Propagat.*, vol. 11, pp. 451–453, Jul. 1963.

[12] K. Sato, *et al.* "Measurement of reflection and transmission characteristics of interior structures of office building in the 60-Ghz band," *IEEE Trans. Antennas Propagat.*, vol. 45, pp. 1783–1791, Dec. 1997.

[13] Naval Air Systems Command "Electronic warfare and radar systems engineering handbook," Washington DC, Apr. 1997.

[14] M. Paulson, S. O. Kundukulam, C. K. Aanandan, and P. Mohanan, "A new compact dual-band dual-polarized microstrip antenna," *Microwave and Optical Technol. Lett.*, vol. 29, no. 5, pp. 315–317, 2001.

[15] W. C. Chan, *Performance analysis of telecommunications and local area networks*. Norwell: Kluwer Academic Publishers, 1999.

[16] Y. Xiao, X. Shen, and H. Jiang, "Optimal ACK mechanisms of the IEEE 802.15.3 MAC for ultra-wideband systems," *IEEE J. Select. Commun.*, vol. 24, no. 4, pp. 836–842, Apr. 2006.

[17] A. Sadri, "802.15.3c Usage model document (UMD), Draft," 15-05- 0055-21-003c, Jan. 2007 (ftp://ieee:wireless@ftp.802wirelessworld.com/15/06/15-06-0055-21-003c-mmwave-802-15-3c-usage-model-document.doc)

A Cross-Layer Neighbor Discovery Algorithm for Directional 60 GHz Networks

Ferhat Yildirim and Huaping Liu

IEEE Trans. on Vehicular Technology

4.1 Abstract

Directional antennas are preferred for efficient wireless communications in the 60 GHz spectrum. The recent efforts to adapt high-data-rate medium access control (MAC) protocols from standards that are designed for operation in the lower frequency bands face challenges in acquiring the location of the nearby devices in a network. In this paper, we propose a cross-layer neighbor discovery algorithm for directional 60 GHz networks to assist the MAC layer in using the directional antennas efficiently. We utilize linear and circular polarization and their different responses to reflection to synchronize the transmitter and the receiver. This difference in response is used to determine if there is a direct path between the transmitter and the receiver. Based on this knowledge, the direction of the neighboring devices is determined through a cyclic scanning. The proposed algorithm is analyzed based on the usage models defined in the standard for 60 GHz networks.

4.2 Introduction

The increasing demand for high-speed wireless networks in recent years and exhaustion of spectrum resources have motivated the use of the higher frequency region of the radio spectrum. The 60 GHz band has recently been explored for high-speed, short-range wireless network applications [1–4]. However, wireless communication using the 60 GHz band faces some challenges that are not present in lower frequency bands. Among these challenges, shadowing is a major one. In lower frequency bands, electromagnetic waves could effectively penetrate through most

obstacles in non-line-of-sight (NLOS) environments, but this is unlikely for 60 GHz signals. In order to mitigate the impact of the increased attenuation, shadowing, and multipaths, communication systems using the 60 GHz band favor narrow-beamwidth antennas in the physical layer, not only to align the signal energy in the appropriate direction for efficient transmission of power, but also to reduce the channel delay spread, and thus intersymbol interference (ISI).

Under the IEEE 802.15.3 High Rate Task Group for Wireless Personal Area Networks (WPAN), an alternative Task Group (TG3c) has been working on a physical (PHY) layer standard for 60 GHz networks that would enable wireless communications with over 2 Gbps data rates [5]. Along with an alternative PHY standard, an alternative medium access control (MAC) layer standard for higher frequency networks is also being developed. The MAC defined in IEEE 802.15.3 is designed to be used with omnidirectional antennas in lower frequency wireless networks. Therefore, IEEE 802.15.3 MAC design needs to be modified for use in 60 GHz networks with directional antennas. Several modifications have been proposed in the literature to adapt IEEE 802.15.3 MAC to the 60 GHz band [6, 7]. In all these attempts, the most challenging problem remains to be the neighbor discovery.

In the traditional MAC design, neighbor discovery is a straightforward process due to the use of omnidirectional antennas. For wireless communication with directional antennas that uses the 60 GHz frequency band, the direction of a node is also needed to effectively communicate with it. Such information is not needed in the traditional MAC with omnidirectional antennas. Therefore, neighbor-discovery

algorithms also need to be modified to acquire the directional information of every neighboring node.

A piconet structure has been assumed for IEEE 802.15.3 WPANs. In such a network, any device can be designated as a PicoNet Controller (PNC) that serves as a central hub to other slave devices [8]. Task Group 3c proposes a set of usage models (UM) for applications of 60 GHz wireless networks that are foreseen to be used in practice [9]. These models are presented in Fig. 4.1. Two of the five usage models are designated as mandatory (UM1 and UM5), which consider only a single link between two devices, where directional information is obtained mostly by external means. Most of the existing research is based on these mandatory models [7], which do not require complex neighbor-discovery algorithms due to the limited number of nodes and links involved.

In this paper, we consider all usage models, where many devices could be present in the network and complex directional communication takes place. We propose a neighbor-discovery algorithm for 60 GHz networks with directional antennas. In this proposed algorithm, we utilize the different responses of electromagnetic waves to reflection at 60 GHz to detect if there is a direct path between the transmitter and the receiver. Such information is used both to select an efficient antenna polarization that reduces the multipath effects and to determine the direction of the receiver. Most existing work assumes that the direction information is known *a priori*. Some research uses GPS on every node [10] or angle-of-arrival (AoA) measurements [11]; however, the former is usually not available in indoor environments and the latter could be either inefficient or too complex. We use a

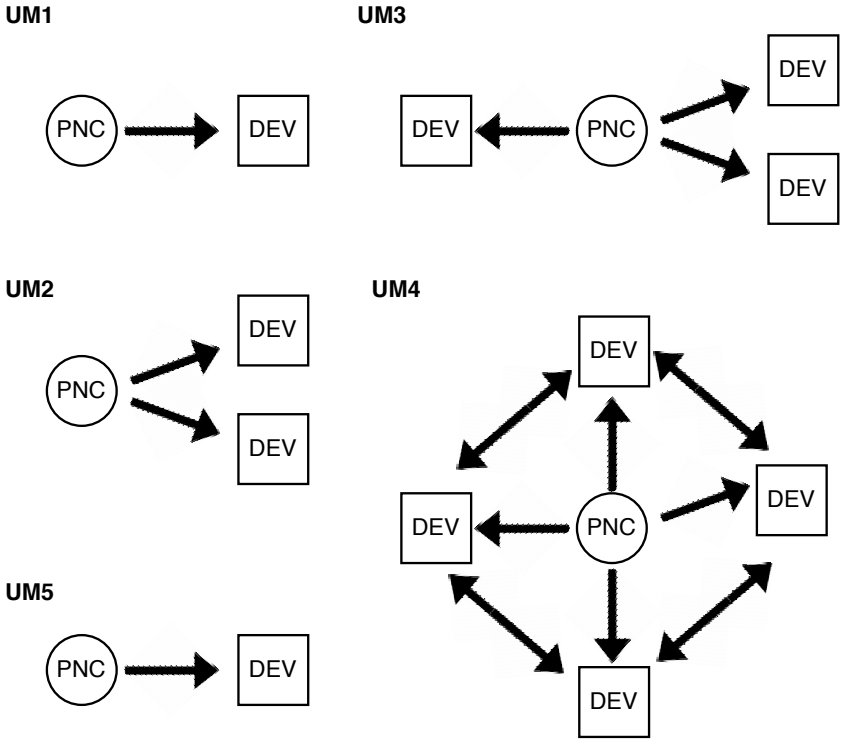

Figure 4.1: Usage models as defined in [9]. UM1, uncompressed video streaming from set-top box to HDTV, and UM5, data download from kiosk to handheld device, is designated as a mandatory usage model; UM2, multiple uncompressed video streaming; UM3, office desktop environment; and UM4, conference room ad-hoc network structure, are designated as optional usage models.

spatial scan based algorithm, which compares the time delay of paths from the transmitter and the receiver. The proposed method is resistant to the fluctuations of the channel.

4.3 Neighbor Discovery for Directional Antennas

In our previous work on improving the performance of the high-speed 60 GHz wireless networks [12], linear and circular polarizations are optimized for use in line-of-sight (LOS) or NLOS propagation conditions to reduce the multipath effects. Based on the results of this study we concluded that in LOS scenarios, circular polarization significantly improves the error performance by decreasing ISI; however, in NLOS scenarios linear polarization performs much better than circular polarization. Therefore, in a 60 GHz network with directional antennas, it is important to have the knowledge of the propagation condition before establishing a link, i.e., if the link between the transmitter and the receiver is LOS or NLOS.

Knowledge of the propagation condition is also important for the proposed neighbor-discovery algorithm with directional antennas. In this section, we briefly discuss the reflection characteristics of polarizations and explain the proposed algorithms for acquiring the LOS/NLOS condition and direction information. We assume that all nodes can use both directional and omnidirectional antennas. Although the data transfer needs to be performed using high gain directional antennas, applications like neighbor discovery will still utilize omnidirectional antennas, for which low data rate is sufficient.

4.3.1 Polarization Effects in 60 GHz Channels

Polarization of an electromagnetic wave is the two-dimensional trace of the electric field vector on the plane that is perpendicular to the direction of propagation. Polarization type is classified based on the shape the electric field traces on this perpendicular plane. If the magnitude ratio of the two orthogonal electric field components is constant and there is no phase difference between these components, the wave is linearly polarized. Two special cases for linear polarization are vertical and horizontal polarizations. On the other hand, when the two orthogonal components have the same magnitude but a 90 degree phase difference, the wave is circularly polarized. Depending on the leading orthogonal component in phase, i.e., direction of rotation, circular polarization is classified into two subclasses: right-hand circular polarization (RHCP) and left-hand circular polarization (LHCP) [13].

The reflection characteristic of circularly polarized waves is quite different from that of linearly polarized waves [14]. For certain incident angles, the handiness of a circularly polarized wave switches upon reflection [15]. Theoretically, a circular polarized antenna rejects a cross polarized incoming wave; in practice, however, the received wave would experience a finite attenuation (e.g., 20 dB [16]). Even with this finite attenuation, appropriate use of polarization could lead to significantly reduced channel delay spread, and hence improved error performance for high data-rate wireless communications.

In LOS environments, the direct path would most likely provide the strongest signal power at the receiver since it has not undergone any reflections and other

losses other than the free-space path loss. The multipaths, on the other hand, are attenuated due to reflections and the longer distance they have traveled through to reach the receiver than the LOS component. The overall attenuation of multipath components could be increased significantly with the use of circular polarization. Depending on the incident angle of each reflection, the handiness of the circular polarization might switch, leading to a greater attenuation at the receiver antenna. This increased attenuation leads to smaller delay spreads, hence a better error performance. In NLOS environments, on the other hand, the communication link depends on the reflected paths between the transmitter and the receiver. In such scenarios, using linear polarization would provide better results than using circular polarization.

Discussion of efficient use of polarization and modification of 60 GHz channel model to incorporate the effects of polarization can be found in [12]. In the next section we use the reflection characteristics of different polarizations to acquire the knowledge of the propagation conditions.

4.3.2 Detection of Presence/Absence of a Direct Path

In order to determine the propagation conditions of the links, we exploit the different reactions of linearly and circularly polarized waves to reflections. Using a dual-polarized antenna [17,18], a test frame is sent in all directions with linear and

circular polarizations with transmit power

$$P_T = P_{T,l} = P_{T,c}, \tag{4.1}$$

where $P_{T,l}$ and $P_{T,c}$ represent the transmit power for linear and circular polarized test frames, respectively. In order to avoid interference, these transmissions may occupy different time slots or different frequency bands. The receiver is also equipped with a dual polarized antenna, which can detect both linear and circular polarized waves; however, the handiness of the circular polarized antenna is inverted with respect to the transmitter antenna in the detection stage. Under this setup, the power of the first received path with linear and circular polarized receive antennas can be written as

$$P_{R,l} = P_{T,l} - L_p - L_{\text{ref}}, \tag{4.2a}$$

$$P_{R,c} = P_{T,c} - L_p - L_{\text{ref}} - K_{\text{cr}}. \tag{4.2b}$$

where L_p is the propagation path loss, L_{ref} is the loss due to possible reflections, and K_{cr} is the cross polarization rejection ratio of the antenna.

In LOS scenarios, it is expected that, the first arrival path is the direct path, hence $L_{\text{ref}} = 0$. Even with a finite K_{cr}, e.g., a typical value of about 20 dB, $P_{R,c}$ is significantly attenuated due to cross handiness. The power difference between the two test frames is expressed as

$$\delta_R = P_{R,l} - P_{R,c}. \tag{4.3}$$

Since the propagation path loss is the same regardless of the polarization of the wave, classification of the communication environment can be easily made: if $\delta_R \leq K_{\mathrm{cr}}$, environment is LOS; otherwise, it is NLOS.

Although the reflection losses to the same path for linear and circular polarizations could differ slightly, this difference is negligible when compared to K_{cr}. This algorithm differentiates LOS and NLOS by detecting the presence or absence of a reflection for the first arrival path using the unique reflection characteristics of circular polarization. The result of this detection is reported back to the transmitter by sending either an ACK/LOS or an ACK/NLOS frame. The transmitter, upon receiving either of the ACK frames, switches the antenna polarization accordingly; circular polarization for LOS, and linear polarization for NLOS.

4.3.3 Detection of Transmission Direction

Once the condition of the wireless channel is determined, the system needs to locate the most efficient direction of transmission to the receiver. This direction should be along the direct path for the LOS case, and the strongest path for the NLOS case. In LOS scenarios, the direct path has a unique time delay, which will be used to identify this particular path. On the other hand, in NLOS scenarios, neither the time delay nor the received power (i.e., measurable quantities at the receiver) are unique. Therefore, a more complex approach is needed for NLOS propagation conditions. One should note that, based on the proposed usage models, LOS communication topology is dominant although NLOS cases still exist.

In order to determine the direction of transmission, we propose a pseudo-synchronization scheme between the transmitter and the receiver to distinguish between the different paths received by the receiver. In this scheme, the transmitter applies a time stamp to every packet it sends according to its local clock. The period of this local clock should be of appropriate length so as not to interfere with several adjacent transmission cycles. Moreover, the resolution of the timer should be high enough to distinguish the shortest time delay, i.e., direct path in the LOS case. High-frequency timers exist with resolutions as high as 13 ps [19], which is enough to detect the difference of time delay in 60 GHz channels where the minimum delay is typically in the order of nanoseconds. If the environment is LOS, the first received path is the most efficient path for communications. The receiver pseudo-synchronizes its internal clock with the time stamp on the received test frame. If the environment is NLOS, the receiver takes the strongest received path as the most efficient path, which is not necessarily the first one received. The shortest reflected path might have a higher reflection loss than a slightly longer reflected path. Upon detecting the incoming test frame, the receiver also pseudo-synchronizes its internal clock with the time stamp on the received frame based on the LOS/NLOS information. In either LOS or NLOS case, after pseudo-synchronization, there will be an offset between the internal clocks of the receiver and transmitter, and this offset corresponds to the propagation delay of the most efficient path. This pseudo-synchronization information is sufficient to find the most efficient direction to the receiver.

We assume that the communication environment is divided into a predefined

number of sectors, each with a certain angular spread (i.e., sectored cell approach). The transmitter sends a probe frame with a time stamp from each sector consecutively in a circular fashion. After transmission in each sector, the transmitter stops and listens for a possible ACK frame from the intended receiver. In this fashion, all the sectors will be swept and all possible directions are covered. The receiver will most likely receive more than one probe frame from different sectors. However, each time a probe frame is received, the time stamp on the frame is compared with the local clock. When the time stamp and the local clock match, the receiver replies with an ACK frame indicating the correct direction of transmission. A matching probe time stamp and receiver internal clock indicates that the transmitter has sent the probe frame using the sector that contains the most efficient path that was detected in the testing/sychnronization process.

The pseudo-synchronization of the transmitter and receiver is illustrated in Table 4.1. At time t_0 the transmitter sends out an omnidirectional test frame with time stamp (according to its internal clock) tx_0. The receiver at t_1 receives this frame and resets its internal clock to tx_0; meanwhile the internal clock of the transmitter has advanced by t_{p1}, the propagation delay of the specific path. After t_d seconds, the transmitter sends out another packet (a probe frame), however, this time using a directional antenna and sweeping through all sectors in the horizontal plane. At time t_n, the instant this transmission occurs, the internal clocks of the transmitter and receiver are $tx_0 + t_{p1} + t_d$ (time stamp on the frame) and $tx_0 + t_d$, respectively. The receiver at t_{n+1} receives this packet after t_{p2}, the propagation delay of the current path. If the transmitter has selected the correct direction to

transmit, t_{p1} would be equal to t_{p2} and the time stamp of the second frame will match the internal clock of the receiver. This will trigger the transmission of an ACK frame by the receiver, indicating that the correct direction of transmission has been found by the transmitter. The data transmission is carried afterwards. In the case of unequal t_{p1} and t_{p2}, the receiver waits for the next probe frame.

This approach works flawlessly in LOS scenarios. However, in NLOS scenarios, since the time delay for each path is not unique, further processing is required. A multipath, which might have experienced several reflections from the transmitter to the receiver, can have the same time delay with another multipath, whose path is completely different from the first one. This is not the case for the direct path in a LOS scenario, since there is only one path going directly from the transmitter to the receiver and it has its own unique time delay. Therefore, in LOS scenarios, once the time stamp matches at the receiver, the transmitter can stop its cyclic scanning since there is no possibility of finding another direct path. In NLOS scenarios, however, even though there is a time stamp match in the receiver, cyclic scanning should be continued until the whole neighborhood is scanned. In order to identify each transmission, a sector ID number is also transmitted within the probe frame. The receiver records the received strength and the sector ID every time the time stamp matches its internal clock. The ID number of the sector that has the strongest reception with the correct time delay is transmitted back to the receiver to indicate the correct direction of transmission. Although very unlikely, it is still possible that two sectors have the same delay and received power characteristics in the NLOS scenario. In such cases, the receiver randomly selects a sector that

Table 4.1: Transmitter-receiver pseudo-synchronization

Time step	Transmitter local clock	Receiver local clock
t_0	tx_0	–
t_1	$tx_0 + t_{p1}$	tx_0
$\vdots$	$\vdots$	$\vdots$
t_n	$tx_0 + t_{p1} + t_d$	$tx_0 + t_d$
t_{n+1}		$tx_0 + t_{p2} + t_d$

has a time delay match and replies back to the transmitter. Since these sectors have the same received power and time delay, any one of them could be used for communication. This directional detection algorithm is further explained in detail in Appendix A.

4.4 Application Scenarios and Performance Analysis

4.4.1 Usage Models

The algorithm outlined in the previous section is a cross-layer process, which communicates with both PHY and MAC layers. It gathers and provides information to both layers. Since this algorithm is optimized for 60 GHz PHY, we assess its performance based on the scenarios that are defined by the IEEE Task Group for 60 GHz wireless communications.

The usage models can be found in [9] and are shown in Fig. 4.1 for convenience. There models are summarized as follows.

- *UM1*: Wireless streaming of uncompressed high-definition video from a source

(set-top box, DVD player, game console, etc.) to a high-definition display device. The nodes are fixed, but the link can be LOS or NLOS, and random shadowing caused by human body is possible. The separation between nodes are 5–10 meters in a typical residential environment. The typical required data rate is 3.56 Gbps for a 1080p (1920x1080 pixels, progressive) image with a color depth of 24 bits and refresh rate of 60 Hz. This usage model is designated as mandatory.

- *UM2*: Wireless streaming of uncompressed high-definition video from a source to multiple display devices, which are seperated by 5 meters. The nodes are fixed, one display has a LOS with the source and the others are NLOS, and random shadowing caused by human body is possible. Video streams to each display are assumed to have a rate of 0.62 Gbps, resolution of 480p (640x480 pixels, progressive), color depth of 24 bits, and refresh rate of 60 Hz. This usage model is designated as optional.

- *UM3*: Wireless personal area networks in a typical office setting. A high-definition display device, which is separated from the computer by 1 meter, has similar link characteristics as UM1. The printer, which has a NLOS link to the computer, is separated by 5 meters. The external storage is assumed to have a LOS link to the computer with a 0.25 Gbps link in both directions. This usage model is designated as optional.

- *UM4*: A wireless ad-hoc network in a conference room setup with a central control hub and a projector display device. Several computer nodes are

available that are assumed to be 3 meters apart from the central hub. The link characteristics between a node and the display device are similar to UM1. A data rate of 0.125 Gbps is assumed between the controller hub and a computer node in both directions. The data rate between the computer nodes is assumed to be 0.0416 Gbps for a separation of 1 meter. In this scenario, all links are assumed to have a LOS link with the hub. This usage model is designated as optional.

- *UM5*: Wireless data download from kiosk to a handheld device over a LOS link with a burst speed of up to 2 Gbps. The user needs to manually adjust the direction of the antennas; hence no neighbor discovery is necessary. This usage model is designated as mandatory.

Depending on the application, a sufficient wireless link can be established using either one or two directional antennas at both ends of the link. For most of the applications, a unidirectional link is sufficient for high-data-rate transmission (e.g., video from player to screen). In such scenarios, only one directional antenna is sufficient at the source of the data that is being transmitted. This would require only a single execution the neighbor-discovery algorithm, since the receiver uses an omnidirectional antenna. However, some applications require simultaneous bidirectional high-data-rate communications (e.g., file server and computer). In such scenarios both nodes need to perform the neighbor-discovery algorithm to steer the directional antennas in the appropriate directions.

Based on the usage models defined above, we can assume that nodes are mostly

stationary or fixed, but change of the channel environment or shadowing by moving human body can alter the physical link characteristics between a transmitter and a receiver. Moreover, the use of both directional and omnidirectional antennas helps reduce the number of neighbor detection execution, hence reducing the overhead.

4.4.2 Performance

In order to analyze the performance of the proposed neighbor-discovery algorithm, we initially consider a single node and random events that might require the execution of the algorithm. This analysis is then expanded to N nodes in the wireless personal area network. However, note that, N can be as low as 2, which is the case for UM1 and UM5.

We study the performance of the proposed algorithm in a node, which can be either a PNC or a slave device. In the sectored spatial domain, let us assume that the probability of the node detecting the neighbor in any sector is p_s. The probability of locating the neighbor in the L-th sector is

$$p_L = p_s(1 - p_s)^{L-1}. \tag{4.4}$$

Let T_t be the time spent during the LOS/NLOS detection phase and T_s be the time spent at each sector for direction detection. The total time spent for detection of the neighbor at the L-th sector is expressed as

$$T_L = T_t + LT_s, \tag{4.5}$$

where the probability of neighbor detection within T_L is defined in (4.4). If we define the maximum number of sectors as N_s, which is related to the beamwidth of the directional antenna, and assume that p_s is uniformly distributed over all sectors, i.e., $p_s = \frac{1}{N_s}$, we can rewrite (4.4) as

$$p_L(l) = \frac{(N_s - 1)^{l-1}}{N_s^l}, \tag{4.6}$$

which is the probability mass function of $T_L, L = 1, \ldots, N$. Fig. 4.2 illustrates this distribution for different values of the antenna beamwidth. The probability of locating the neighbor at time T_L decreases as the beamwidth decreases and as L increases. This is expected for a scanning algorithm. Several existing works have proposed a random search algorithm for neighbor discovery using directional antennas [20]. However, this would yield to a more complex algorithm. The probability distribution in Fig. 4.2 suggests that it is more likely that the location of the neighbor is detected in the earlier stages of the scanning algorithm compared to the later steps of the scanning process. In the limiting case, where there is only one sector, i.e., omnidirectional case, the probability of locating the neighbor in that first (and only) sector is 1.

In the case that the neighbor is LOS with the node, the neighbor is detected at time T_L with a probability $p_L(L)$. However, if the neighbor is NLOS, as explained in the previous section the node has to go through all the sectors before detecting the direction of the neighbor. Therefore, the detection happens at time T_L, where $L = N_s$, with a probability of 1.

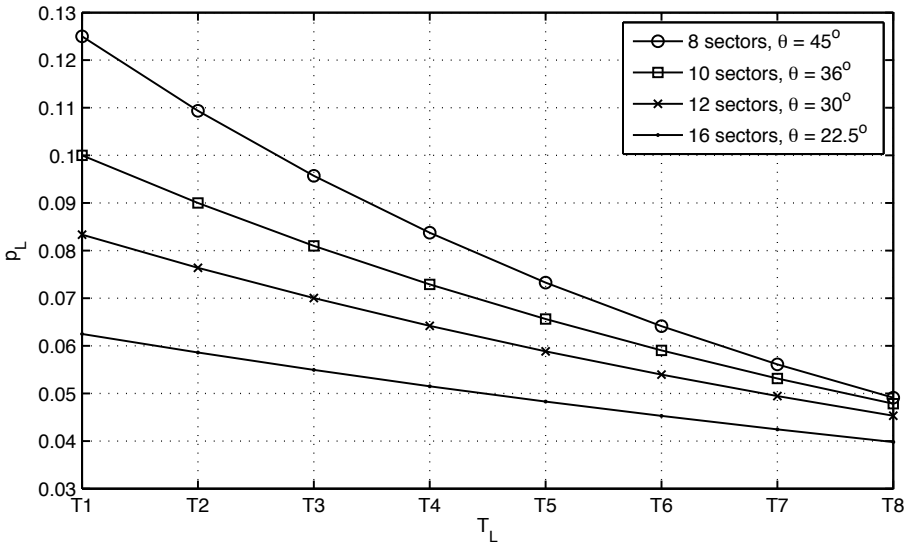

Figure 4.2: Probability of detecting the neighbor in the L-th section at time T_L. The location of the neighbor is assumed to be uniformly distributed around the node. The distribution shown here corresponds to a LOS scenario, where, once the neighbor is detected, the neighbor-discovery algorithm terminates and data transfer begins.

Once the neighbor is detected, the node can either continue to detect other possible neighbors or start transmission of data packets. It is possible that at any random time instant, the neighbor or the node itself changes location, the link between the node and the neighbor becomes obstructed, the channel environment changes, or a new neighbor joins the network. Under such circumstances, a new neighbor detection might be required. The occurrence of an event is random and independent from other events. We assume that the occurrence of such event is a Poisson process with a rate λ. These events can occur anytime during the operation of the network and are independent of one another. For such Poisson process, if $n(t)$ represents the number of events that occurred up to time t, then $n(b) - n(a)$

corresponds to the number of events that occurred between time b and a and has a Poisson distribution expressed as

$$P[(N(t+\tau) - N(t)) = k] = \frac{e^{-\lambda\tau}(\lambda\tau)^k}{k!}, \tag{4.7}$$

where k is the number of events that occurred in time frame τ. For the time duration of τ, under a constant network load, the time allocated for neighbor discovery can be defined as kT_L, and the time allocated for the information transfer is $\tau - kT_L$. We define the time allocation ratio of the network as

$$\eta = \frac{kT_L}{\tau}, \tag{4.8}$$

where 100η represents the percentage of time allocated for the neighbor-discovery algorithm.

In LOS scenarios, T_L represents the detection time that occurred at the L-th sector. However, for the performance analysis, we assume that detection always occurs at the last available sector, i.e, $L = N_s$, creating an upper bound on η. On the other hand, in NLOS scenarios, T_L is already defined with $L = N_s$. The probability mass function of (4.8), $P[\eta = x]$, after extracting k from (4.8), can be expressed as

$$P\left[k = \frac{\tau x}{T_L}\right] = \frac{e^{-\lambda\tau}(\lambda\tau)^{\frac{\tau x}{T_L}}}{(\frac{\tau x}{T_L})!}. \tag{4.9}$$

Note that k represents the number of occurred events and is a positive integer. This distribution is illustrated in Fig. 4.3. We vary the event occurrence rate

Table 4.2: Parameters of 60 GHz network and channel used in the simulation of neighbor detection

Parameter	Value
Size of ACK, L_a	14 bytes
Size of probe L_f	14 bytes
Propagation delay, t_p	9.4 ns
Channel listening delay, t_l	$\sim 2t_p$
Base rate, R_b	54 Mbps
Data rate, R_d	1 Gbps
Transmission duration, τ	1 s
Number of sectors	8

from 1 event/s to 100 events/s. Although the usage models described at the beginning of this section define mostly stationary networks, we test the performance of the neighbor detection algorithm in extreme cases. The parameters that are used in this analysis are listed in Table 4.2. In this simulation, we assume that the LOS/NLOS detection duration, T_t, consists of one test frame and one acknowledgement frame at the base rate transmitted with omnidirectional antennas and their corresponding propagation delays. Similarly, the scan duration, T_s, is assumed to consist of a probe frame at the base rate transmitted with a directional antenna, its propagation delay, and the channel listening period for possible acknowledgement from the neighbor.

We observe in Fig. 4.3 that when the event rate increases, λ, the time allocated to the neighbor discovery algorithm also increases. Such behavior is expected with an increased number of algorithm execution triggering event occurrences. However, one should note that, in the very extreme case of 100 events per second, the time

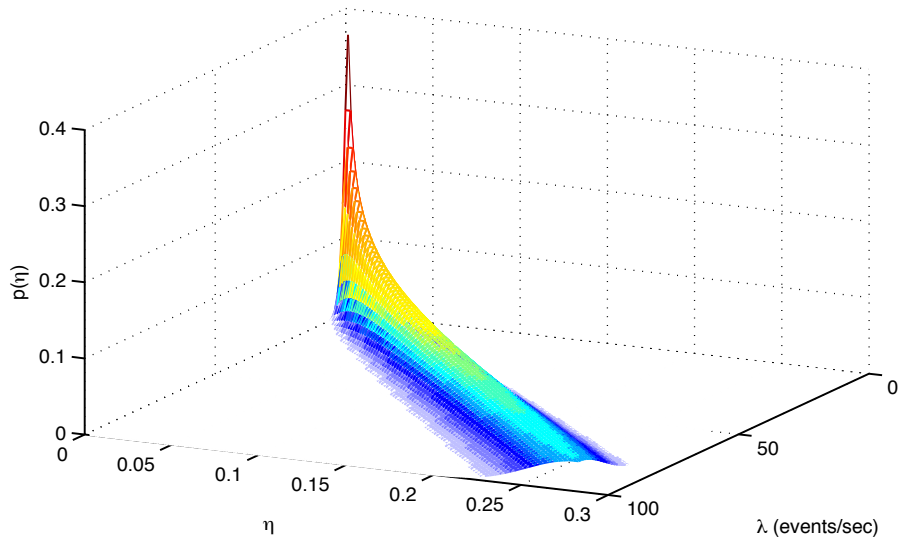

Figure 4.3: Probability of η, the time allocation ratio of the network, with changing rate of event occurrence that triggers the execution of the neighbor-discovery algorithm. The event rate, λ, is defined as the number of events per second. Events could be, but are not limited to, relocation of nodes, change in channel environment, or addition of new nodes to the network. A large λ corresponds to a highly dynamic network environment.

allocated for the proposed algorithm is less than 30%. Such event rate is unrealistic for the defined usage models and is studied only to observe the variable η in extreme conditions. In a more modest, but still highly dynamic network with $\lambda = 10$, the allocated time is less than 10%. In such a network, assuming that the transfer rate is set for 1 Gbps, with the introduction of the neighbor-discovery algorithm, the data rate is reduced to 0.9 Gbps in the worst-case scenario.

Fig. 4.4 shows a snapshot of the analysis in Fig. 4.3 with different event rates and number of nodes. In order to establish an upper bound for the time allocation ratio of the network in the multiple-node network scenario, we assume that every

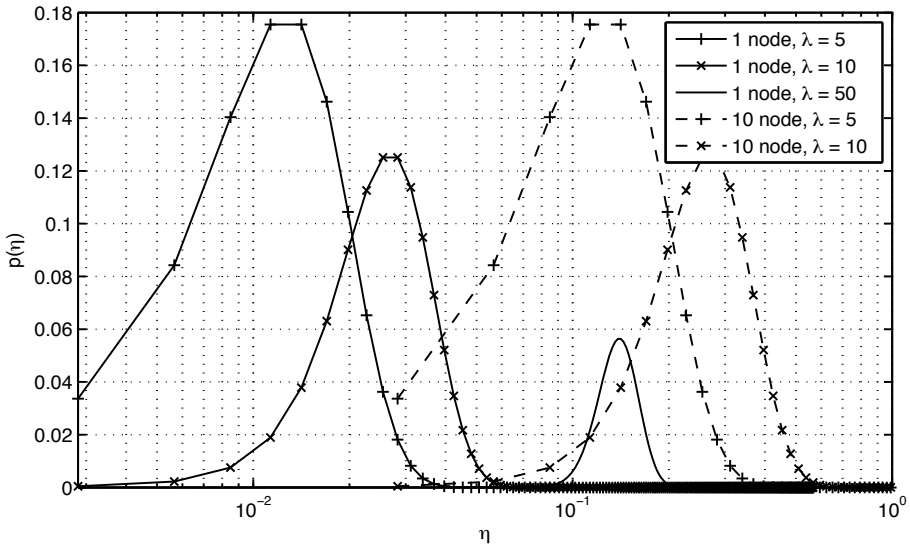

Figure 4.4: A snapshot of the probability of η for different event occurrence rates with a single node and 10-node network. The increase in the node count also increases the time allocated for the neighbor-detection algorithm. In this simulation, we assume a worst-case scenario, where every node performs a neighbor discovery and updates its information when an event occurred and made one node execute the algorithm. Under such scenario we observe the upper bound on the time allocated for the neighbor-discovery algorithm.

node executes the neighbor-discovery algorithm when an event occurs. The result of such event might not require the execution of the algorithm on every node; however, by doing so, we obtain the upper bound on the time allocation ratio of the network. From Fig. 4.4 we observe that by increasing the number of nodes the time allocated for the neighbor discovery algorithm increases up to 40% depending on the event occurrence rate.

In practical wireless networks for all usage model scenarios, an event rate of 1 or 2 events per second is expected given that the most frequent change might happen with the movement of human bodies, either carrying a node or obstructing a path.

Considering this, our analysis shows that even for a 10-node network, which might be considered a highly populated network according to the usage models, under the worst-case scenario, the time allocated for the neighbor-discovery algorithm is less than 10%. Moreover, such overhead might be compensated by the use of the polarization scheme explained in [12] without increasing the complexity, since LOS/NLOS topology information is obtained as a part of the neighbor-discovery process.

4.5 Conclusion

We have developed a neighbor-discovery algorithm for wireless communication networks with directional antennas operating in the 60 GHz band. This algorithm is a cross-layer scheme to effectively locate the neighbors around a device. It efficiently exploits the unique behaviors of different polarizations in LOS and NLOS environments for improved performance. A novel approach for detecting the presence or absence of a direct path between the transmitter and the receiver is proposed, which is used to determine if the communications link is LOS or NLOS. Through the overhead and efficiency analysis, we have observed that even in highly populated and very dynamic networks, the time allocated for the neighbor-discovery algorithm does not exceed 10% in the worst-case scenario. Considering the significant increase in the physical-layer performance as a result of the efficient use of an appropriate polarization for each specific propagation scenario, this decrease in the network performance is expected to be compensated by the suppressed ISI

and the reduced error rates.

Bibliography

[1] P. F. M. Smulders, "Exploiting the 60 GHz band for local wireless multimedia access: prospects and future directions," *IEEE Commun. Mag.*, vol. 40, pp. 140–147, Jan. 2002.

[2] C. J. Gibbins, "Radiowave propagation in the 30-60 GHz band," *IEE Colloquium Radiocomm. in the Range 30-60 GHz*, pp. 1/1-1/4, Jan. 1991.

[3] S. Geng, *et al.* "Millimeter-wave propagation channel characterization for short-range wireless communications," *IEEE Trans. Veh. Technol.* , vol.58, no.1, pp.3–13, Jan. 2009.

[4] T. Manabe, *et al.* "Polarization dependence of multipath propagation and high-speed transmission characteristics of indoor millimeter-wave channel at 60 GHz ," *IEEE Trans. Veh. Technol.*, vol. 44, no. 2, pp. 268–274, May 1995.

[5] S. Yong, "TG3c channel modeling sub-committee final report," *IEEE 802.15-07-0584-00-003c*, Jan. 2007 (https://mentor.ieee.org/802.15/file/07/15-07-0584-01-003c-tg3c-channel-modeling-sub-committee-final-report.doc).

[6] A. Xueli and R. Hekmat, "Directional MAC protocol for millimeter wave based wireless personal area networks," in *Proc. IEEE VTC-Spring 2008*, May 2008, pp. 1636–1640.

[7] F. Kojima, C. W. Pyo, Z. Lan, H. Harada, S. Kato, and H. Nakase, "Necessary modifications on conventional IEEE802.15.3b MAC to achieve IEEE802.15.3c millimeter wave WPAN," in *Proc. IEEE PIMRC 2007*, Sep. 2007, pp. 1–5.

[8] IEEE. Std. 802.15.3-2003 ed. Wireless Medium Access Control (MAC) and Physical Layer (PHY) Specifications for High Rate Wireless Personal Area Networks (WPANs).

[9] A. Sadri, "802.15.3c Usage model document (UMD), Draft," 15-05- 0055-21-003c, Jan. 2007 (ftp://ieee:wireless@ftp.802wirelessworld.com/15/06/15-06-0055-21-003c-mmwave-802-15-3c-usage-model-document.doc)

[10] R. R. Choudhury, X. Yang, R. Ramanathan, and N. H. Vaidya, "Using directional antennas for medium access control in ad hoc networks," in *Proc. ACM MobiCom*, Sep. 2002, pp. 59–70.

[11] N. S. Fahmy, T. D. Todd, and V. Kezys, "Ad hoc networks with smart antennas using IEEE 802.11-based protocols", in *Proc. IEEE Int. Conf. Commun.*, Apr. 2002, pp. 3144–3148.

[12] F. Yildirim, A. S. Sadri, and H. Liu, "Polarization effects for indoor wireless communications at 60 GHz," *IEEE Commun. Lett.*, vol.12, no.9, pp.660-662, Sep. 2008.

[13] C. A. Balanis, *Advanced engineering electromagnetics*. New York: Wiley, 1989.

[14] I. Katz, "Radar reflectivity of the ocean surface for circular polarization," *IEEE Trans. Antennas Propagat.*, vol. 11, pp. 451–453, Jul. 1963.

[15] K. Sato, *et al.* "Measurement of reflection and transmission characteristics of interior structures of office building in the 60-Ghz band," *IEEE Trans. Antennas Propagat.*, vol. 45, pp. 1783–1791, Dec. 1997.

[16] Naval Air Systems Command, "Electronic warfare and radar systems engineering handbook," Washington DC, Apr. 1997.

[17] Y.-P. Hong, J.-M. Kim, S.-C. Jeong, D.-H. Kim, and J.-G. Yook, "Low-profile S-band dual-polarized antenna for SDARS application," *Antennas and Wireless Propagat. Lett.*, vol. 4, pp. 475–477, Jan. 2005.

[18] M. Paulson, S. O. Kundukulam, C. K. Aanandan, and P. Mohanan, "A new compact dual-band dual-polarized microstrip antenna," *Microwave and Optical Technol. Lett.*, vol. 29, no. 5, pp. 315–317, 2001.

[19] J. Jansson, A. Mantyniemi and J. Kostamovaara, "A delay line based CMOS time digitizer IC with 13 ps single-shot precision," in *Proc. IEEE ISCAS'05*, May 2005, pp. 4269–4272.

[20] Z. Zhang, "Performance of neighbor discovery algorithms in mobile ad hoc self-configuring networks with directional antennas," in *Proc. IEEE MILCOM*, Oct. 2005, pp. 3162–3168.

Network Analysis of Direction Detection Scheme for 60 GHz Wireless Communication Networks

Ferhat Yildirim and Huaping Liu

5.1 Abstract

Due to the characteristics of electromagnetic waves at 60 GHz, directional antennas are favored in this spectrum for their ability to focus the transmitted power in a desired direction. However, use of directional antennas also increases the complexity of the system, and requires advanced direction detection algorithms to locate the receivers in the neighborhood. Based on our novel direction detection scheme, in this paper, we analyze the effects of this increased complexity on the network performance. We derive the statistics of random events that might happen during the normal operation of the network and using this information we obtain the normalized throughput of a dynamic network, which uses the proposed direction detection scheme.

5.2 Introduction

The introduction of 60 GHz wireless communication standard by IEEE 802.15 Task Group 3c opened up numerous opportunities for applications that can utilize high-speed wireless communication in a license-free channel [1]. Although, the increase in frequency enables the high data rate communication, it also causes problems that originate from the unique characteristics of electromagnetic waves in high frequency spectrum. One of the significant differences of high-frequency bands in comparison to lower frequency channels is the increased attenuation of electromagnetic waves, which makes them to travel shorter distances and prevents them to penetrate objects. The most effective method to mitigate this effect is to

use directional antennas.

Directional antennas, with increased antenna gain, can focus the transmitted energy towards the intended recipient and not only mitigate the disadvantages of 60 GHz channel, but also increase the spatial efficiency of the channel. A network of nodes that are equipped with directional antennas can simultaneously access the channel given that each direction of transmission does not block another transmission.

However, use of directional antennas also increases the complexity of the network. One drawback with directional antennas is that the transmitter needs to locate the receiver to steer its antenna pattern to achieve the desired optimum transmission efficiency. If we assume a sectored cell spatial allocation scheme, where the neighborhood is divided into predefined number of angular sectors, the transmitter needs to identify the sector at which the recipient is located. This is a challenging process, especially in dynamic wireless networks.

Many authors, whose research is based on directional antennas assume that the location information is available to the transmitter by external means such as a GPS data [2, 3]. In our previous study [5], we proposed a cross-layer direction detection algorithm that can efficiently locate the recipient. We utilize a cyclic scanning algorithm, in which transmitter scans all sectors to locate the receiver. An increase in the number of sectors causes an increase in the antenna gain (which is tied to the antenna beamwidth), reduction in error-rate and increase in performance. However, more sectors also result in increased scanning time allocation, which in turn reduces the overall throughput of the network. Such trade-off be-

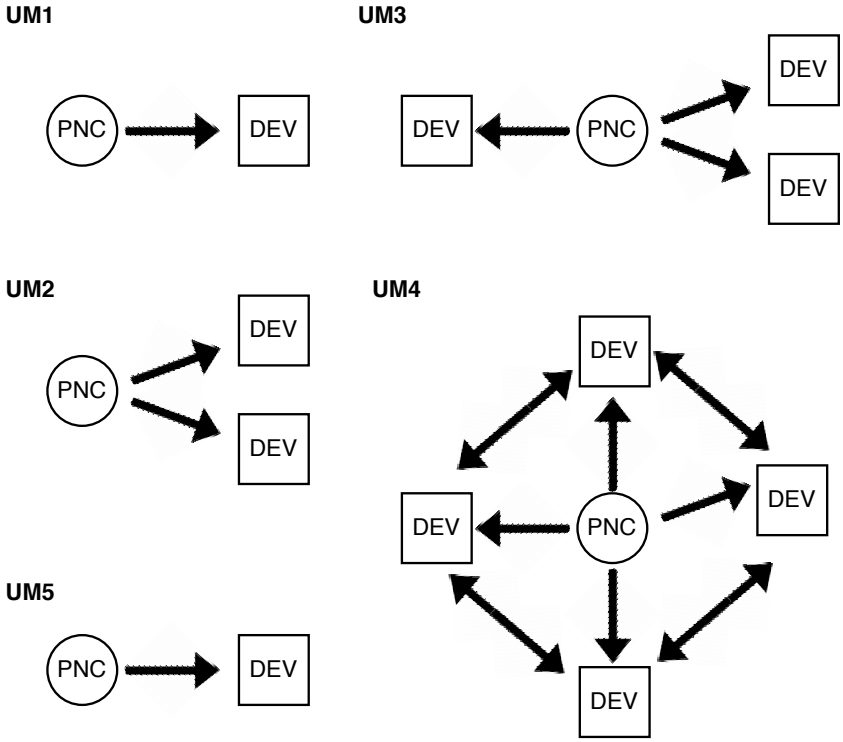

Figure 5.1: UM1, uncompressed video streaming from set-top box to HDTV, and UM5, data download from kiosk to handheld device, is designated as a mandatory usage model; UM2, multiple uncompressed video streaming; UM3, office desktop environment; and UM4, conference room ad-hoc network structure, are designated as optional usage models.

tween number of sectors and network performance has been studied in [5].

In this paper, we analyze the proposed direction detection scheme in a network environment. We derive the statistics of the time that is allocated to the execution of the direction detection scheme based on the assumptions of 60 GHz channel parameters. We consider random events that might trigger the execution of the direction detection scheme such as relocation of nodes, signal obstruction or new

data transmission request. We further derive the throughput of the network under these random events, and re-execution of the direction detection algorithm. We present our results using the usage models (UM) defined in the IEEE 802.15.3c document [6]. These analysis and results would provide a complete picture for the use of directional antennas in 60 GHz wireless networks in dynamic indoor networks.

5.3 Directional Communication in 60 GHz Channel

Among the five proposed usage models by IEEE 802.15 Task Group 3c that are illustrated in Fig. 5.1, two of them are designated as mandatory. In addition to the usage models, several channel models for 60 GHz PHY are also proposed in the standard [6]; some of which are associated with the usage models. The usage models and their associated channel models are listed in Table 5.1. All models assume indoor scenarios with relatively stationary nodes. The structure of the network is neither ad-hoc, nor infrastructure. Although any device can communicate with another one, the link can be established without any hops or intermediary nodes.

Depending on the application, a sufficient wireless link can be established using either one or two directional antennas. In the majority of the usage models, a unidirectional link is sufficient for high-data-rate transmission (e.g., video from player to screen). In such scenarios, only one directional antenna is sufficient at the source of the data that is being transmitted. Such configuration requires only one

Table 5.1: Usage Models and Simulation Environments

UM1	Point to point video	Residential LOS
UM2	Point to multi-point video	Residential LOS and NLOS
UM3	Wireless desktop	Desktop LOS and NLOS
UM4	Conference	Office LOS
UM5	Kiosk	Kiosk LOS

direction detection scheme to be executed since receiver would be using an omnidirectional antenna. However, some applications require simultaneous bidirectional high-data-rate transmission such as data transfer from/to an external storage. In such scenarios, both nodes need to perform a direction detection scheme to steer their antenna in the appropriate direction.

During the normal operation of a network, random events such as addition or removal of nodes, change of location and number of nearby scatterers (including users), transmission requests and relocation of nodes can occur. Each of these events may change the distribution of the network in such a way that nodes need to re-detect the transmission direction. In this paper, we investigate the performance of the network under such events and the efficiency of the direction detection scheme with varying number of nodes in the network. In our analysis we assume that MAC layer would handle any packet collisions, channel access and problems that arise from directional antennas (such as deafness) since these are beyond the scope of this paper.

5.4 Network Analysis

For our analysis, we assume a simple model for the transmitter antenna pattern that is expressed as

$$D(\beta) = \begin{cases} G, & |\beta| < \phi/2 \\ 0, & \text{otherwise,} \end{cases} \tag{5.1}$$

where ϕ is the antenna beamwidth in degrees, D is the antenna pattern in both the horizontal and vertical planes, and G is the fixed gain of the antenna in dBi, which can be defined as,

$$G = 10 \log_{10} \left(\frac{360}{\phi} \right). \tag{5.2}$$

Using the pattern given in (5.1) and (5.2), we can define an antenna by specifying only the antenna beamwidth. The beamwidth of the directional antenna is associated with the angular spread of the sector in sectored cell deployments, and is eventually related to the number of sectors, which is $N_s = \frac{360}{\phi}$.

5.4.1 Event Rate Estimation

Let us assume that N is a random variable that represents the sector number at which the receiver is discovered, when using the cyclic scanning algorithm of the direction detection scheme. If the probability of a node detecting the receiver in any sector is p_s, then we can express the probability of detecting the receiver as,

$$p_N = p_s(1 - p_s)^{N-1}. \tag{5.3}$$

Let T_s be the time spent during the synchronization of the transmitter and the receiver and T_d be the time spent at each sector for direction detection. The total time spent for detection of a neighbor is expressed as

$$T_N = T_s + NT_d. \tag{5.4}$$

If we assume that p_s is uniformly distributed over all sectors, i.e., $p_s = \frac{1}{N_s}$, we can rewrite (5.3) as

$$p_N(n) = \frac{(N_s - 1)^{n-1}}{N_s^n}, \tag{5.5}$$

which is the probability mass function of N. In the case that the nodes are in LOS with each other, the recipient is detected at time T_N with a probability p_N. However, if the recipient is NLOS, based on direction detection algorithm, the transmitter has to go through all the sectors before detecting the direction of the recipient. Moreover, the detection happens after the scan of last sector, $N = N_s$, with a probability of one. Once the receiver is detected, the transmitter can start the transmission of data packets.

As discussed earlier, it is possible that at any random time instant, a node can change location, the link can become obstructed, the channel environment can change, or a new node can join the network. Under such circumstances, a new direction detection might be required. We assume that the occurrence of such event is a Poisson process with a rate λ. These events can occur anytime during the operation of the network and are independent of one another. For such Poisson process, if $e(t)$ represents the number of events that occurred up to time t, then

$e(b) - e(a)$ corresponds to the number of events that occurred between time b and a and has a Poisson distribution expressed as

$$P[(e(t+\tau) - e(t)) = k] = \frac{e^{-\lambda\tau}(\lambda\tau)^k}{k!}, \tag{5.6}$$

where k is the number of events that occurred in time frame τ. For the time duration of τ, under a constant network load, the time allocated for neighbor discovery can be defined as $L_m k T_N$, where L_m is the number of nodes communicating. Note that, L_m is usually two, based on the usage models defined by Task Group 3c. Therefore, if bidirectional transmission is employed, each node has to re-detect the transmission direction, hence the total direction detection time increases by L_m-fold. We define η, the time allocation ratio of the channel, as the ratio of time spent during direction detection to the total operation time. This can be expressed for a two node network as,

$$\eta = \frac{L_m k T_N}{\tau}, \tag{5.7}$$

where $L_m = 2$.

In a more populated network environment, when an event occurs, it is not necessary that all nodes in the network are effected, hence, re-detecting the transmission direction is unnecessary for all nodes of the network. This can be modeled by assigning different event rate, λ, to each node of the network. The events still follow a Poisson process as defined in (5.6), however each node has different rate, which creates a random distribution of event frequency and occurrence time among

all nodes. We can rewrite (5.7) for a general network case as

$$\eta = \frac{L_m}{\tau} \sum_{i=1}^{L} k_i T_{N,i}, \tag{5.8}$$

where L represents the total number of nodes in the network. Note that, the total time for detection, T_N, which is also a random variable, is expected to change with different nodes, hence included in the summation.

5.4.2 Throughput

The throughput of a system is calculated as the ratio of the successfully transmitted bits to the total transmission time. Normalized throughput (S_n), on the other hand, is defined as the ratio of the throughput to the data rate, R_d. In the calculation of throughput, we also take in to account of overhead that arises from the use of direction detection scheme by utilizing the random variable η, which is defined in the previous section.

For an ideal error free channel, a longer data frame would increase the throughput, however, for a typical indoor wireless channel, where both noise and ISI are present, it is impossible to achieve such a relation. In data critical applications, a single bit error in the entire data frame might require the retransmission of that frame, assuming that there is no data recovery scheme employed. In streaming applications, on the other hand, although some level of error can be tolerated, too many error bits also require the retransmission of the packet to keep the quality

Table 5.2: Channel Parameters used in Simulation

Parameter	Residential	Library	Hallway
Path loss exponent	1.53	3	2.29
Free space path loss intercept (dB)	75.1	50	69.7
Cluster arrival rate (1/ns)	1/4.76	0.25	1
Ray arrival rate (1/ns)	1/1.30	4	1
Cluster decay factor	4.19	12	1
Ray decay factor	1.07	7	7
Mean number of clusters	4	17	1

of service high.

In the direction detection scheme that we introduced earlier, the cyclic scanning of each sector introduces additional processing time, where no data is transmitted. However, the information obtained from the cyclic scanning enable the transmitter to beamform along the optimum direction for communication. This would increase the received power and SNR at the receiver side, which in turn decreases the probability of error and allows longer data frames to be sent. Therefore, one needs to choose the data frame length in such a way that it is not too long to create too many retransmissions or too short to create inefficiency by underutilizing the channel resources.

For a bit sequence of length d, the probability of successful transmission is

$$p_s = (1 - p_e)^d, \tag{5.9}$$

where p_e is the probability of an erroneous bit, i.e., BER. Using (5.9) the normalized

throughput, in its raw state, can be written as,

$$S_N = \frac{d}{R_d}\frac{p_s}{t}, \tag{5.10}$$

where t is the total transmission time. In a previous study, [7] showed that

$$\lim_{d\to 0} S_n = 0, \tag{5.11}$$

and

$$\lim_{d\to \infty} S_n = 0, \tag{5.12}$$

and there exists a d_{opt}, optimum data frame length, for a given BER value. The corollary of [7] is intuitive since, in a non-ideal channel, i.e., non zero BER, as $d \to \infty$, it would be impossible to transmit any successful frame. Similarly, as $d \to 0$, we are not transmitting any data, hence $S_N \to 0$. However, it is not practical to obtain a statistical value for d_{opt} since it depends on the wireless environment and its error performance.

In order to obtain a more general normalized throughput expression, we also need to consider the time spent during the direction detection, where no data is transmitted. This would decrease the throughput since within a certain amount of time, the amount of total transferred data decreases. Therefore, for a total operation time of τ, the throughput needs to be scaled with $(1 - \eta)$ in order to include the effect of direction detection scheme. Moreover, one also needs consider the increasing number of nodes in a network environment to obtain a general

expression for the normalized throughput of a network of L nodes. The throughput of the network scales with the number of communications channels, i.e., L/L_m, since each communication channel increases the data transferred in a given time interval.

Moreover, the total operation time, t, can be expressed as,

$$t = \frac{d/R_d}{(1-\eta)}, \tag{5.13}$$

where d/R_d is the time required to transmit data stream d. Substituting (5.13) back into (5.10), applying network scaling, which is discussed before, and further normalizing due to scaling of network nodes leads to

$$S_N = (1-\eta)p_s, \tag{5.14}$$

which represents the general form of normalized throughput for a network of L nodes.

5.5 Results

In this section, we analyze the statistical nature of the normalized throughput, which is derived in the previous section, in a network environment with varying number of nodes. For this analysis, we set bit-error-rate and optimum data frame length to constant values since we will observe the stochastic nature of the throughput relatively. In other words, we would be able to observe the trend of

the throughput as the number of nodes in the network changes, rather than the absolute throughput of a specific network. All random parameters, such as number of events, are drawn based on their probability distribution; a large sample set and a statistical average would yield reliable results for desired throughput analysis.

5.5.1 Bit-Error Performance

In order to find the bit-error-rate, we performed error performance simulation based on the channel environments that are defined in the IEEE 802.15.3c. We have selected to simulate the most common environments that are presented in Table 5.1 using a BER simulator in LOS scenario. The parameters of the channel models are listed in Table 5.2, and the results are presented in Fig. 5.2.

Although modulation using orthogonal frequency division multiplexing (OFDM) is widely used in wireless communications, because of the varying inter-ray arrival times, we modulate the data using a set of orthogonal sinusoids over a block interval, very similar to OFDM algorithm. However, this method allows us to sample the received signal at any sampling interval.

For the channel models proposed in IEEE 802.15.3c, a 0.1 ns sampling interval appears to be enough in order to detect most of the rays. Using this sampling interval, we quantize the excess delay of every ray to the nearest sampling point. A total of 10^4 different channel impulse response realizations are used in the simluation. Other simulation parameters are listed in Table 5.3. Note that, since we are interested in the raw error performance, typical communications blocks such

Table 5.3: Simulation Parameters

Parameter	Value
Modulation	BPSK
Number of channel realizations	10,000
Number of OFDM block per realization	100
Number of subcarriers per OFDM block	128
Data rate	1 Gbps
Sampling interval of complex sinusoids	0.1 ns

as an interleaver and channel encode are not included.

5.5.2 Optimum Data Frame Length

Using the BER simulation results of Fig. 5.2, we calculate the optimum data frame length, d_{opt}. We assume that the antenna gain, transmit power and path loss are such that the BER is always lower than 10^{-2} for the omnidirectional case, and considering a 4 sector channel, the receiver is always on the last scanned sector. The SNR and BER is calculated using the gain introduced by the 90^o directional antenna. The distribution of normalized throughput with respect to data frame length is presented in Fig. 5.2. Furthermore, Table 5.4 presents the optimum data length size for various channel models and number of sectors. Note that, the optimum data length would not be effected by the number of nodes, as the PHY parameters would be same regardless of number of nodes around.

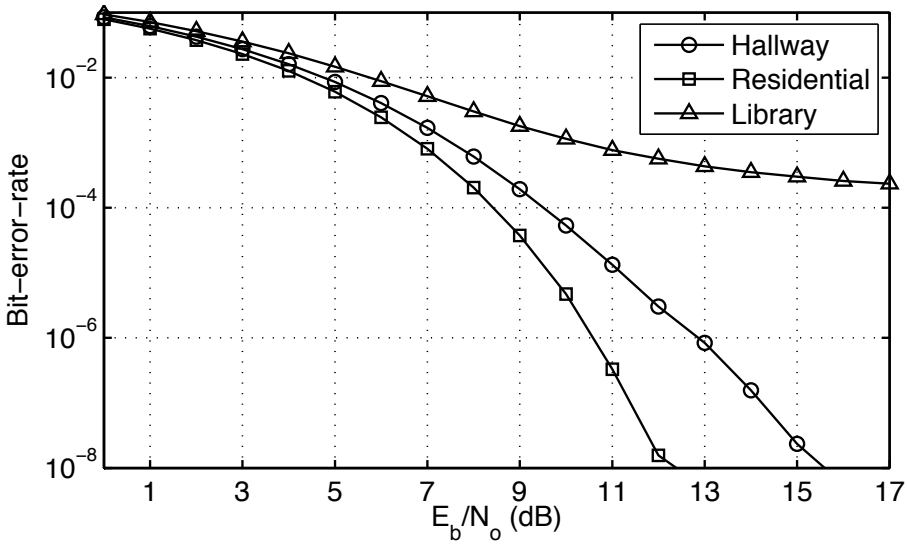

Figure 5.2: Bit-error-rate performance of three indoor environments that are defined in IEEE 802.15.3c. A LOS channel is assumed.

Table 5.4: Optimum Data Frame Length in Bytes

Number of Sectors	2	4	6	8
Residential	145	7128	157K	711K
Library	67	205	321	378
Hallway	188	3819	20K	52K

5.5.3 Event Rate and Time Allocation Ratio

It is expected that an increase in the number of nodes would adversely effect the efficiency of the network. We analyze the time allocation ratio of a dynamic network using (5.8). Figure 5.4 presents the time allocation percentage of a network with changing number of nodes in the network, while comparing 4 and 8 sector deployment. In order to achieve a statistically true analysis, we sample 10^3 different

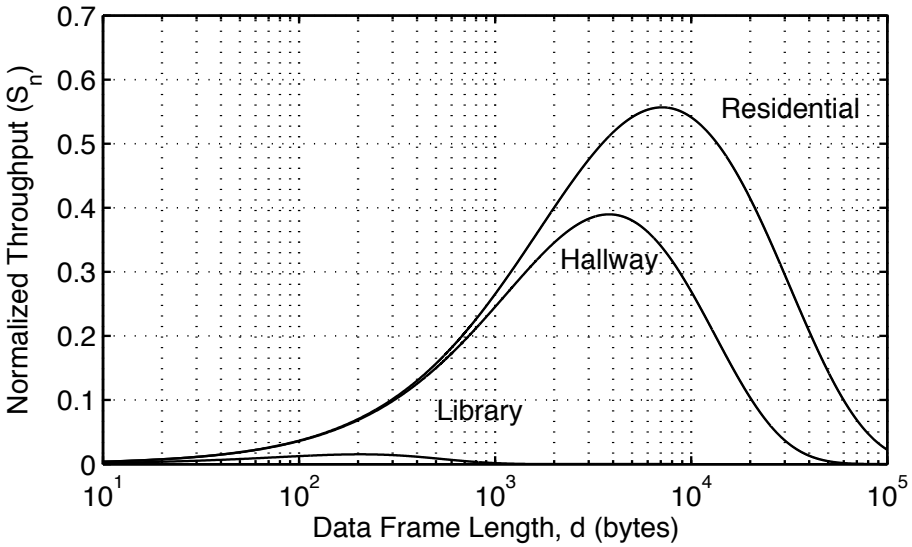

Figure 5.3: Optimum data frame length for a 4 sector scenario in three indoor environments that are defined in IEEE 802.15.3c. Notice that as multipath density decreases - as in residential environment - the optimum data frame length increases.

η value for each selection of number of nodes. Number of events in time interval τ, i.e., k, is drawn from a Poisson distribution. Similarly, the detection time, T_N, is also drawn based on its random distribution. For simplicity, we selected $\tau = 1s$, without loss of generality. The three curves for each number of sectors corresponds to the event rate of , $\lambda = 1, 10, 100$ events per second, from bottom to top, respectively.

A lower number of sectors means fewer sectors to scan, hence the time spent on direction detection is lower for 4 sector scenario when compared to the 8 sector scenario. However, note that, 4 sector scenario uses directional antennas that has wider beamwidth in comparison to the 8 sector scenario; this leads to lower spatial efficiency and more importantly lower gain, transmit power and SNR, which in turn

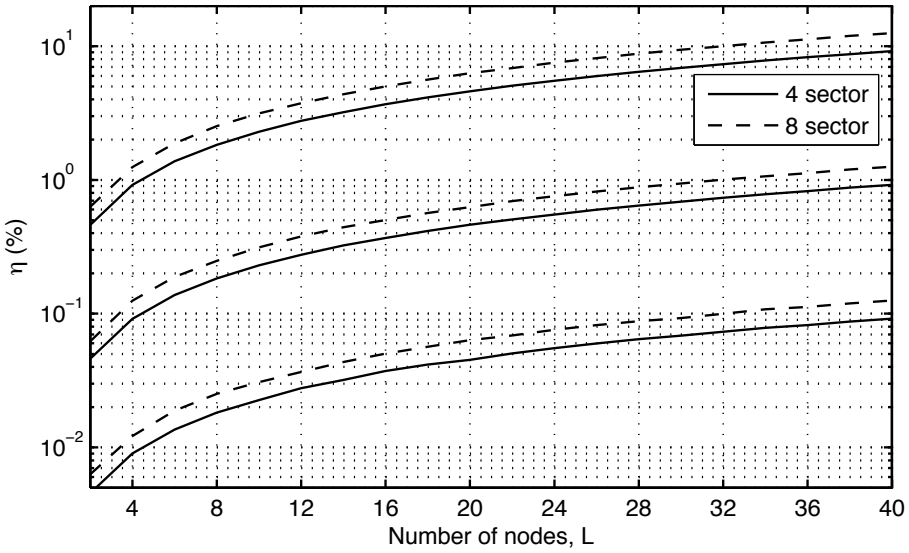

Figure 5.4: Time allocation percentage for 4 and 8 sector scenario with different event rates. Three curves represents event rate of $\lambda = 1, 10, 100$ events per second from bottom to top, respectively. Note that practical event rate for defined usage model lies between 1–10 events per second, 10 events per second representing a highly dynamic channel.

increases the error rate. The tradeoff between error rate and number of sectors has been studied in our previous work [5].

An increased event rate also increases the time allocation ratio, which is expected. The highest time allocation percentage is observed for a 8 sector scenario in a network with 40 nodes, which is slightly over 10%. Even with 100 events per second, which is not nearly practical for 60 GHz usage models, only 10% of the transmission time is lost to the direction detection scheme. Considering this is a very extreme case and typical values of time allocation is less than 1%, we can easily claim that the overhead introduced by the directional detection scheme does not effect the network performance significantly.

5.5.4 Normalized Throughput

The true metric to asses the performance of the network with the utilization of direction detection scheme is to study the normalized throughput. Absolute throughput is expected to increase with the increasing number of nodes in the network, since more data can be transferred in the same time interval with more communication channel present in the environment. However, the normalized throughput is scaled both for data rate and number of communication channels so that one can observe the trend with changing number of nodes in the network, which utilizes direction detection.

We select constant values for BER and data frame length in order to compare the normalized throughput for different indoor environments. We assume that, BER is just below 10^{-2} when using an omnidirectional case, and obtain the BER for SNR that corresponds to the power amplification due to the increased antenna gain in a 8 sector approach. The data frame length is selected based on the study in the previous section and Table 5.4.

Figure 5.5 shows the normalized throughput for the three indoor environments that are defined in the IEEE 802.15.3c. Although there is a very small decline in the normalized throughput with the increasing number of nodes in the network, it can be regarded as constant for all scenarios. The vast difference between the normalized throughput of indoor environments arises from the difference in their corresponding BER, which in turn is related with the channel environment and multipath density. The library environment, due to excessive reflections and ob-

structions from shelves and other furniture, has a very high BER and low throughput when compared to other environments.

However, the most important conclusion out of this analysis is the fact that the increase in the number of nodes in the network, eventhough the time allocation ratio increases, has no practical influence on the overall normalized throughput of the system. In other words, when the proposed direction detection scheme is deployed in a dynamic network, a size increase would not pose a problem in the network performance that originates from the complexity increase due to the use of the proposed direction detection scheme. One should note that, since it is beyond the scope of this paper, we do not consider the MAC layer for our throughput study. Introduction of directional antennas requires complex MAC approach and would be the main reason for the bottleneck in the network performance as size of the network grows bigger.

5.6 Conclusion

In this paper, we analyzed the direction-detection scheme that we introduced earlier in a network environment. We statistically derive a relation for the events that might happen during the normal operation of the network that might require the re-detection of the direction of the receiver. We have shown that this re-detection does not clog the network by taking up too much time even in the extreme cases of a very crowded network and 100 events per second. We also derived a general expression for the normalized throughput of a network, which uses directional

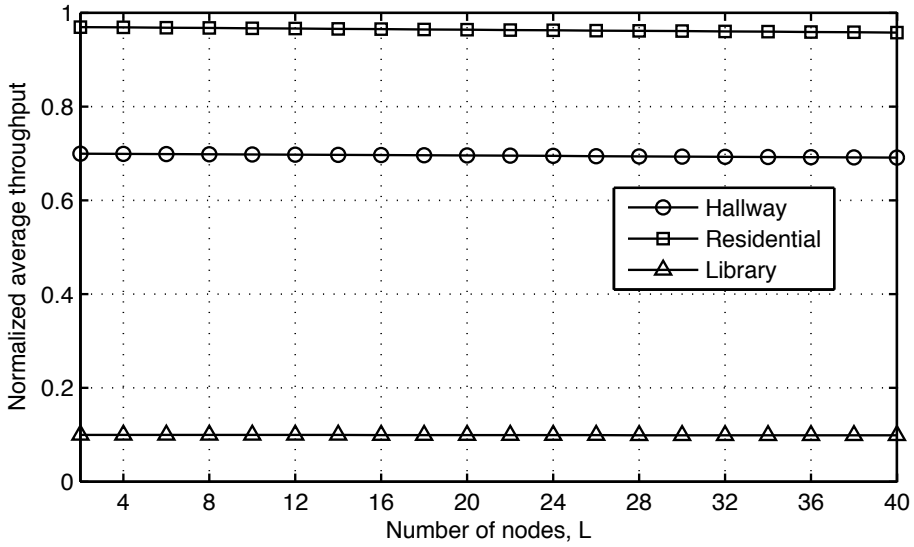

Figure 5.5: Normalized throughput for three indoor environments that are defined in IEEE 802.15.3c. The BER, data frame length are set deterministically to compare the performance of the network with growing number of nodes in a 8 sector scenario.

antennas on both ends of the communication channel. From the BER and optimum data frame length analysis, we study the trend of the normalized throughput in a growing network of nodes. Based on this analysis, we can conclude that direction-detection will not be the bottleneck in the performance when a dynamic and growing network is considered.

Bibliography

[1] P. F. M. Smulders, "Exploiting the 60 GHz band for local wireless multimedia access: prospects and future directions," *IEEE Commun. Mag.*, vol. 40, pp. 140–147, Jan. 2002.

[2] R. R. Choudhury, X. Yang, R. Ramanathan, and N. H. Vaidya, "Using directional antennas for medium access control in ad hoc networks," in *Proc. ACM MobiCom*, Sep. 2002, pp. 59–70.

[3] N. S. Fahmy, T. D. Todd, and V. Kezys, "Ad hoc networks with smart antennas using IEEE 802.11-based protocols", in *Proc. IEEE Int. Conf. Commun.*, Apr. 2002, pp. 3144–3148.

[4] A. Sadri, "802.15.3c Usage model document (UMD), Draft," 15-05- 0055-21-003c, Jan. 2007 (ftp://ieee:wireless@ftp.802wirelessworld.com/15/06/15-06-0055-21-003c-mmwave-802-15-3c-usage-model-document.doc)

[5] F. Yildirim and H. Liu, "A cross-layer neighbor discovery algorithm for directional 60 GHz networks," to appear in IEEE Transactions on Vehicular Technology, 2009.

[6] S. Yong, "TG3c channel modeling sub-committee final report," *IEEE 802.15-07-0584-00-003c*, Jan. 2007 (https://mentor.ieee.org/802.15/file/07/15-07-0584-01-003c-tg3c-channel-modeling-sub-committee-final-report.doc).

[7] Y. Xiao; X. Shen; H. Jiang, "Optimal ACK mechanisms of the IEEE 802.15.3 MAC for ultra-wideband systems," *IEEE J. Select. Commun.*, vol. 24, no. 4, pp. 836–842, Apr. 2006.

A Practical Double Directional Channel Model for 60 GHz Wireless Communication Networks

Ferhat Yildirim and Huaping Liu

6.1 Abstract

We propose a modified channel model for 60 GHz wireless systems that include the effects of directional antennas and polarization. We study the statistics of the angular parameters of the channel model and simplify an existing channel model for practical applications. The effects of antenna beamwidth in commonly encountered scenarios are investigated. The results can be used as the basis for cost analysis. We also simulate the performance of the channel and compare our results with non-directional transmission.

6.2 Introduction

Directional transmit and receive antennas could be used to compensate for the high signal loss of communications using the 60 GHz spectrum. Through directional antennas, the signal energy is aligned for transmission at the appropriate direction for spatial division to increase network efficiency. Directional antennas also reduce the channel delay spread, hence the intersymbol interference (ISI) for high-speed applications. For complete characterization of directional channels, an appropriate channel model is required, which is more mathematically intensive than their omnidirectional counterparts.

Under the IEEE 802.15.3 High Rate Task Group for Wireless Personal Area Networks (WPAN), an alternative Task Group (TG3c) has been working on a physical layer (PHY) standard for 60 GHz channel that would enable wireless communications with over 2 Gbps data rate [1]. However, this model includes only

time-of-arrival and direction-of-arrival (DoA) parameters. This is not sufficient for networks with directive transmit and receive antennas of various beamwidth.

In this paper, we provide a channel model for 60 GHz wireless networks with directional transmit and receive antennas that utilize different polarizations. The proposed model is based on IEEE 802.15.3c channel model and completes the missing scenarios of this model for 60 GHz communications. However, such a model, where each path is defined by its attenuation, time delay, and transmit and receive angles, is too complex for use in practical simulation scenarios. Therefore, we derive the statistical behavior of the angular parameters of each ray, which leads to a simplified channel model that considers both transmitter and receiver directionality. The simplified model is practical for use in simulation studies.

Moreover, the effects of antenna beamwidth on the multipath density for the scenarios defined in the IEEE standard are studied. This helps gain insights on the angular properties of indoor environments and for choosing an appropriate antenna type and beamwidth, which is crucial for optimizing the performance and cost of the antenna system. Finally, we study the performance of the directional channel under several scenarios defined in the IEEE standard to support the topics studied in this paper.

6.3 Double-directional channel model

6.3.1 IEEE channel model for 60 GHz spectrum

Several channel models (e.g., [1, 4–6]) and measurement results (e.g., [7–9]) for 60 GHz wireless communications channel can be found in the literature; the most comprehensive one is the IEEE 802.15.3c model [1]. This model is based on the well known Saleh-Valenzuela multipath model [10], whose impulse response is expressed as

$$h(t) = \sum_{l=0}^{L-1} \sum_{k=0}^{K_l-1} \alpha_{k,l} \delta(t - T_l - \tau_{k,l}), \tag{6.1}$$

where L is the number of clusters, K_l is the number of rays in the l-th cluster, $a_{k,l}$ is the gain of the k-th ray in the l-th cluster, T_l is the arrival time of the first ray in the l-th cluster, and $\tau_{k,l}$ is the delay of the k-th ray within the l-th cluster relative to the first arrival path of that cluster. The delay of the first ray received, i.e., T_0, is assumed to be zero, as well as the reference point in each cluster, i.e., $\tau_{0,l} = 0$.

In order to study the performance of networks with directional antennas, IEEE 802.15.3c Task Group extended the model in (6.1) to include the DoA parameters. Measurement campaigns performed under IEEE 802.15.3c indicate that rays arrive in clusters not only in time, but also in angle [9]. Therefore, the modified model can be written as

$$h(t, \phi) = \sum_{l=0}^{L-1} \sum_{k=0}^{K_l-1} \alpha_{k,l} \delta(t - T_l - \tau_{k,l}) \delta(\phi - \Phi_l - \phi_{k,l}), \tag{6.2}$$

where Φ_l is the mean angle of arrival of the l-th cluster and $\phi_{k,l}$ is the angle of

arrival of the k-th ray from the l-th cluster. Similar to the previous case, $\Phi_0 = 0$, marking the first arrival path as the reference path. The probability density of $\phi_{k,l}$ is expressed as

$$p(\phi_{k,l}) = K \exp(f(\phi_{k,l})), \tag{6.3}$$

where K is a normalization factor and function $f(\cdot)$ depends on the scenario [11]. Based on the measurement procedures described in [12, 13], the IEEE 802.15.3c Task Group concludes that a Gaussian distribution is best suited for indoor environments in 60 GHz for $p(\phi_{k,l})$ expressed in (6.3).

6.3.2 Double-directional channel model

Although the channel model proposed by IEEE contains DoA information, it still lacks the direction-of-departure (DoD) information, which makes the model incomplete. A double-directional channel model that includes both DoA and DoD information is essential for performance evaluation of a wireless system that utilizes directional antennas.

In [14], the effects of antenna and the propagation channel itself are separated by introducing the following definitions: the *propagation channel* is described by the double-directional channel response, excluding both the transmit and receive antennas; the *radio channel* is described by a non-directional channel response that includes both antennas; in between these two is the *single-directional* channel. This is illustrated in Fig. 6.1. Using these definitions as reference, the IEEE 802.15.3c channel model described in the previous section can be classified as a

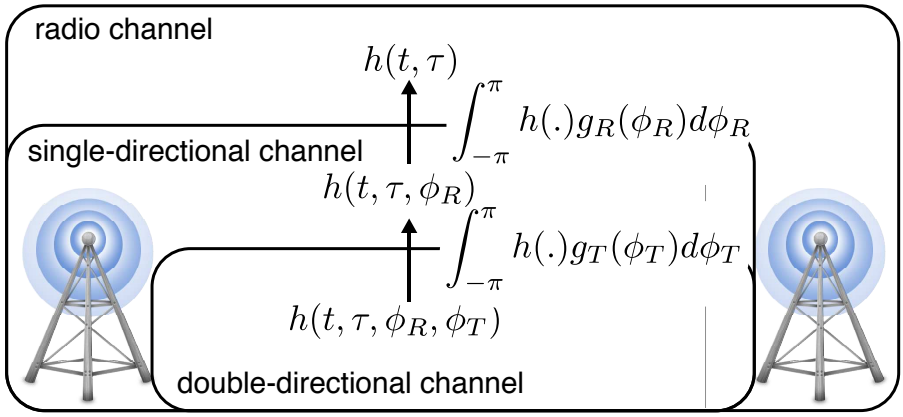

Figure 6.1: Relation between channel representations, where $g_T(\phi)$ and $g_R(\phi)$ represents the antenna for transmitter and receiver antenna, respectively.

singe-directional channel response, which only considers the DoA statistics, that is, the transmit antenna is considered omnidirectional.

Using the same notation of (6.1) and (6.2), the impulse response of the double-directional channel with N resolvable paths can be expressed as

$$h(\tau,\phi_R,\phi_T)=\sum_{i=1}^{N} A_i\delta(\tau-\tau_i)\delta(\phi_R-\phi_{R,i})\delta(\phi_T-\phi_{T,i}), \tag{6.4}$$

where A_i is the complex gain for each path; $\phi_{R,i}$ and $\phi_{T,i}$ are the DoA and DoD for each path, respectively. In general, all parameters A_i, τ_i, $\phi_{R,i}$, $\phi_{T,i}$, and the total number of resolvable paths N depend on the absolute time t. For slowly fading channels (e.g., indoor environments), we can assume that all of these parameters are static, i.e., independent of time, hence the omission of variable t in (6.4).

Since rays arrive in cluster both in time and angle in the 60 GHz channel, the SV model needs to be modified to make it a double-directional propagation channel

model similar to (6.4). Such an impulse response that considers the clustering behavior of rays can be written as

$$h(t,\phi_T,\phi_R) = \sum_{l=0}^{L-1}\sum_{k=0}^{K-1} \alpha_{k,l}\delta(t - T_l - \tau_{k,l}) \times\delta(\phi_T - \phi_{k,l,\mathrm{DoD}})\delta(\phi_R - \phi_{k,l,\mathrm{DoA}}) \tag{6.5}$$

where we have replaced τ in (6.4) with t. The parameters of (6.5) are defined as following:

- $\alpha_{k,l}$: complex multipath gain coefficient for the k-th ray of the l-th cluster
- T_l: arrival time (delay) of the first ray of the l-th cluster
- $\tau_{k,l}$: the delay of the k-th ray of the l-th cluster relative to T_l
- $\phi_{k,l,\mathrm{DoA}}$: direction of arrival for k-th ray of the l-th cluster
- $\phi_{k,l,\mathrm{DoD}}$: direction of departure for k-th ray of the l-th cluster.

By definition, $T_0 = \tau_{0,l} = 0$; therefore, the excess delay is given as

$$\varepsilon_{k,l} = T_l + \tau_{k,l}. \tag{6.6}$$

Following the approach in [15], we can construct the DoA and DoD parameters

similar to (6.6) as

$$\phi_{k,l,\mathrm{DoA}} = \theta_R + \delta_{l,\mathrm{DoA}} + \varphi_{k,l,\mathrm{DoA}} \tag{6.7a}$$

$$\phi_{k,l,\mathrm{DoD}} = \theta_T + \delta_{l,\mathrm{DoD}} + \varphi_{k,l,\mathrm{DoD}} \tag{6.7b}$$

where reference is selected as the broadside of each antenna.

When comparing (6.7a) and (6.7b) with (6.6), one should note that the values of angular parameters can be negative but time is always positive. In (6.7a) and (6.7b), θ_R and θ_T are the angles between the transmitter-receiver LOS and the broadside of the antenna pattern, respectively; $\delta_{l,\mathrm{DoA}}$ and $\delta_{l,\mathrm{DoD}}$ are DoA and DoD for the first ray of the l-th cluster with respect to θ_R and θ_T, respectively; and $\varphi_{k,l,\mathrm{DoA}}$ and $\varphi_{k,l,\mathrm{DoD}}$ are the offset angles for the k-th ray of the l-th cluster with respect to $\delta_{l,\mathrm{DoA}}$ and $\delta_{l,\mathrm{DoD}}$, respectively.

We assume that $\phi_{k,l,\mathrm{DoA}}$ and $\phi_{k,l,\mathrm{DoD}}$ are mutually independent and they are both independent of ToA parameter $\varepsilon_{k,l}$. Introducing correlation into $\phi_{k,l,\mathrm{AoA}}$, $\phi_{k,l,\mathrm{AoD}}$ and $\varepsilon_{k,l}$ is possible, but this will result in a very complex model [15]. Note that $\theta_R = \theta_T = 0$ since the direction of both transmitter and receiver antennas could be aligned by using methods such as the one summarized in our previous work [3]. We further assume that $\delta_{l,\mathrm{DoA}}$ and $\delta_{l,\mathrm{DoD}}$ are independent random variables and are uniformly distributed over $[-\pi, \pi]$.

Due to the independence of $\phi_{k,l,\mathrm{DoA}}$, $\phi_{k,l,\mathrm{DoD}}$, and $\varepsilon_{k,l}$, the results of the measurement campaigns conducted through the IEEE standards activities can be reused here. In other words, we can assume a Poisson distribution for the ToA param-

eter and a Gaussian distribution for the DoA parameter. Moreover, due to the reciprocity theorem of antennas, we can also assume Gaussian distribution for the DoD parameter.

Using the relations shown in Fig. 6.1 to calculate the radio channel response from the propagation channel response (6.5), we obtain

$$h(t) = \sum_{l=0}^{L-1} \sum_{k=0}^{K-1} \alpha_{k,l} \delta(t - \varepsilon_{k,l}) g_T(\phi_{k,l,\mathrm{DoD}}) g_R(\phi_{k,l,\mathrm{DoA}}). \tag{6.8}$$

If we define the directional gain for each ray which also includes the effects of polarization as

$$A_{k,l}^D = \alpha_{k,l} q_m g_T(\phi_{k,l,\mathrm{DoD}}) g_R(\phi_{k,l,\mathrm{DoA}}), \tag{6.9}$$

then the double-directional channel model can be expressed as

$$h(t) = \sum_{l=0}^{L-1} \sum_{k=0}^{K-1} A_{k,l}^D \delta(t - \varepsilon_{k,l}). \tag{6.10}$$

In an LOS scenario, we can rewrite the channel impulse response as

$$\begin{aligned} h(t) &= a_{\mathrm{LOS}} q_0 g_T(\phi_{\mathrm{LOS,AoD}}) g_R(\phi_{\mathrm{LOS,AoA}}) \\ &\quad + \sum_{l=0}^{L-1} \sum_{k=0}^{K-1} A_{k,l}^D \delta(t - \varepsilon_{k,l}) \end{aligned} \tag{6.11}$$

where $\phi_{\mathrm{LOS,DoA}}$ and $\phi_{\mathrm{LOS,DoD}}$ are, respectively, the DoA and DoD for the LOS path. The polarization factor q_m and the index m is detailed in [2]. Note that, when $g_T(\cdot)$ is replaced by 1, i.e., with an omnidirectional antenna, the proposed channel

model defined in (6.11) simplifies to the single-directional channel model that is proposed by IEEE 802.15.3c Task Group and presented in [16].

6.4 Simplified Channel Model

The double-directional channel model given in (6.11) is mathematically complex to be treated as a general model since the patterns of the transmit and receive antennas are countless. Although it seems to be impossible to derive a general directional channel model without removing the effects of directional antennas, an approximate directional channel model can be derived for specific scenarios such as those proposed for IEEE 802.15.3c. It is anticipated that the majority of practical usage of 60 GHz wireless networks would take place in one of the five different indoor scenarios [1]. Therefore, working with an approximate channel model that is generalized specifically for these indoor scenarios would provide enough accuracy while keeping the complexity of the analysis to minimum.

6.4.1 60 GHz specific assumptions

In order to reduce the complexity of the double-directional channel model we consider the indoor scenarios defined in the IEEE 802.15.3c proposal. It has been noted in the proposal that in most of the scenarios, LOS communications is considered over NLOS communications, for both practical and technical reasons. Moreover, we have concluded in our previous work [2] that using circular polarization in

NLOS communications would decrease the performance of the wireless system. Therefore, we also consider only the LOS communications in the indoor scenarios for the simplification of the double-directional channel model.

We specifically focus on three of the five scenarios proposed by IEEE 802.15.3c: residential, library and hallway. The detailed description of each scenario along with their derived channel parameters can be found in [1]. We also assume an uniform sectored antenna with horizontal beamwidth θ_b and gain G. Such antenna pattern is highly preferred in indoor environments for spatial diversity and can be approximated to its ideal pattern using multiple antenna elements. Based on the statistical distribution of DoD and DoA, we can claim that rays that fall within the beamwidth of the antenna will be amplified by a gain factor G, and those fall outside the antenna beamwidth $[-\theta_b, \theta_b]$ will be eliminated. Although in practice elimination is not the case, the combined attenuation from the antenna pattern, increased free space, and reflection loss in 60 GHz channels would render those rays that fall outside of the antenna beamwidth practically eliminated. Under these assumptions, the challenge for reducing the complexity of the double-directional channel model lies in deriving the statisti cal behavior of DoD and DoA.

6.4.2 DoA and DoD statistics in 60 GHz channels

We have discussed that the channel model in (6.11) assumes a uniform distribution for mean cluster angle, and Gaussian distribution for intra-cluster angles. In other words, the proposed channel model, based on the measurement results, provides

only the statistical distribution of DoA and DoD for individual clusters, which is sufficient for establishing an SV model. However, for our studies we need the statistical distribution of the entire DoA and DoD in order to simplify the double-directional channel model in (6.11). The entire angular data is composed of a combination of smaller clusters, whose statistical distribution is known. This can be expressed as

$$\phi \approx \bigcup_{l=1}^{L} \left(\phi_l \sim \mathcal{N}(\mu_l, \sigma_l^2) \right) \tag{6.12}$$

where ϕ is either DoD or DoA distribution; ϕ_l is either DoD or DoA distribution of the l-th cluster with mean μ_l and variance σ_l^2. Note that (6.12) does not represent a summation or multiplication of different random variables. For this reason, deriving a general statistical distribution for ϕ is not possible. However, through a simple derivation it can be shown that

$$\mu = \frac{1}{L} \sum_{l=1}^{L} \mu_l, \tag{6.13}$$

where μ is the mean of ϕ. Since μ_l is a random variable uniformly distributed over $[-\pi, \pi]$, for large L values we can assume that $\mu = 0$. If we consider ϕ as the combination of $\phi_l, l = 1, \cdots, L$ expressed as

$$\phi = \begin{bmatrix} \phi_1 & \phi_2 & \cdots & \phi_L \end{bmatrix}, \tag{6.14}$$

then we can write the variance estimate as

$$\mathrm{Var}(\phi) = \frac{1}{L}\Bigg[\frac{1}{N_1}\sum_{n=1}^{N_1}(\phi_{1,n}-\mu)^2 + \frac{1}{N_2}\sum_{n=1}^{N_2}(\phi_{2,n}-\mu)^2 + \cdots + \frac{1}{N_L}\sum_{n=1}^{N_L}(\phi_{L,n}-\mu)^2\Bigg], \tag{6.15}$$

which, when submitted $\mu = 0$, simplifies to

$$\mathrm{Var}(\phi) = \frac{1}{L}\Bigg[\sum_{l=1}^{L} E[\phi_l^2]\Bigg]. \tag{6.16}$$

Rearranging the expected value and summation yields

$$\mathrm{Var}(\phi) = \frac{1}{L}E\Bigg[\sum_{l=1}^{L} \phi_l^2\Bigg]. \tag{6.17}$$

We substitute a new variable Φ in the equation as

$$\mathrm{Var}(\phi) = \frac{\sigma^2}{L}E[\Phi], \tag{6.18}$$

where

$$\Phi = \sum_{l=1}^{L}\left(\frac{\phi_l}{\sigma}\right)^2, \tag{6.19}$$

is a noncentral chi-square random variable. Using the statistical properties of such distribution, we can calculate the variance in (6.16) as

$$\mathrm{Var}(\phi) = \sigma^2 + \frac{1}{L}\sum_{l=1}^{L}\mu_l^2, \tag{6.20}$$

where the first part is the variance of one cluster and the second part is variance of a uniformly distributed random variable.

Further investigation of the distribution of ϕ reveals that it resembles a uniform distribution over $[-\pi, \pi]$ with some leakage across the limits. A closer look at the variance defined in (6.16) reveals that this leakage is due to the first part of the variance, whereas the second part contributes to the uniform distribution nature of the random variable ϕ. Considering the 2π periodic behavior of the angles, this leakage is expected to smooth out the uniform distribution. Therefore, for large values of L, we can assume that the statistical distribution of ϕ converges to uniform distribution over $[-\pi, \pi]$. This will be further analyzed in the next section. In other words, we can establish the probability of existence for a path between the transmitter and the receiver as

$$p_e = \frac{\theta_b}{\pi}, \tag{6.21}$$

where θ_b is the bandwidth of the sectored antenna.

Based on these assumptions we can rewrite a simplified channel model for 60 GHz as

$$h(t) = a_{\mathrm{LOS}} q_0 G^2 + \sum_{l=0}^{L-1} \sum_{k=0}^{K-1} A_{k,l}^{D} \delta(t - \varepsilon_{k,l}), \tag{6.22}$$

where

$$A_{k,l}^{D} = \alpha_{k,l} q_m p_{e,\mathrm{Tx}} p_{e,\mathrm{Rx}}, \tag{6.23}$$

where $p_{e,\mathrm{Tx}}$ and $p_{e,\mathrm{Rx}}$ are defined by (6.21) for the transmitter antenna and the receiver antenna, respectively.

6.5 Analysis

6.5.1 Angular analysis of IEEE defined scenarios

In the previous section, we derived that the combination of Gaussian random variables with the same variance and uniformly distributed mean could be assumed to have a uniform distribution. Fig. 6.2 shows such distribution for several scenarios defined in the IEEE 802.15.3c document. The leaked tails outside of the limits that we have discussed in the previous section are clearly visible; however, when we consider the 2π periodicity of ϕ, these tails add up to both ends of the $[-\pi, \pi]$ domain, making the overall distribution even closer to uniform. In other words, the first term in (6.16), which causes these tails, vanishes and integrates into the second term due to the periodic behavior of the random variable ϕ. Fig. 6.2 supports the assumption of choosing a uniform distribution for the statistics of random variable ϕ.

Note that uniform distribution of ϕ means that every path has an equal probability of having a DoD or DoA to be a specific angle regardless of the attenuation on that path. However, attenuation plays a significant role on the amount of ISI and the BER performance. Some paths might be attenuated below the noise floor due to the presence of obstacles in the environment, antenna pattern or reflective

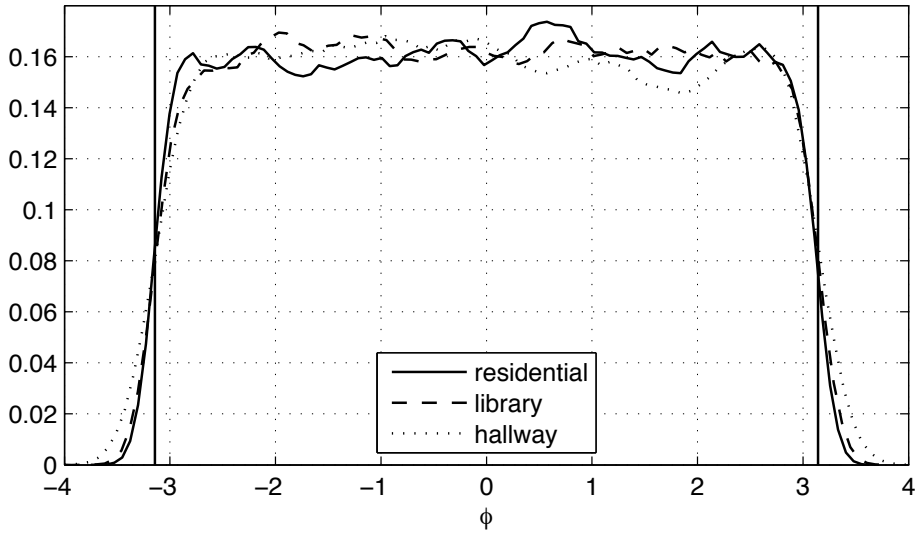

Figure 6.2: Probability density of random variable ϕ for different scenarios defined in IEEE 802.15.3c document. The distribution can be assumed to be uniform, which implies that a path has an equal probability of having a specific DoD and DoA. Note that the leakage outside of the $[-\pi, \pi]$ would be rolled back and further smooth out the uniform distribution.

losses. For practical simulations, such paths will be disregarded as they do not pose any significant impact on ISI and performance. In that respect, we define a parameter called multipath density as the ratio of the average number of the multipaths that can reach the receiver with a strength above the noise floor after the attenuation from antenna pattern and/or polarization effects to the number of all possible multipaths regardless of any attenuation. Note that an LOS component is assumed to exist between the transmitter and the receiver.

Fig. 6.3 compares the multipath density for the three scenarios of interest with respect to the antenna beamwidth. In the ideal case of no obstruction, perfectly symmetrical environment and no attenuation, this relation is expected to increase

linearly; however due to the complex distribution of reflective surface in each scenario we obtain unique characteristics for each environment that is defined in the IEEE 802.15.3c report. For this analysis, we assume a uniform sectored antenna of unity gain (i.e., $G = 1$) to extract the effects of gain increase with respect to omnidirectional antennas. Using a unit gain directional antenna enables us to determine the effects of directional transmission with a fair comparison to omnidirectional transmission. In comparison to the omnidirectional case, which uses only linear polarization, using directional antenna outperforms in every scenario regardless of the use of an appropriate polarization. Moreover, it is clearly seen that an appropriate polarization for a specific channel condition decreases the multipath density significantly.

In addition to the performance improvement with the use of directional antennas, in Fig. 6.3, we also observe that the hallway scenario has a highly directional nature judged by the significant reduction in the multipath density when directional antennas are used. However, such significant reduction in multipath density can not be seen in the library scenario, where a lot of reflective obstacles are present, e.g., bookshelves. Nevertheless, it is clear, especially in the library scenario, that a decrease in antenna beamwidth does not necessarily cause a significant decrease in the multipath density.

Directional antennas that would be used in 60 GHz indoor wireless systems are likely going to be array antennas, where configuration of the array is modified to form a particular antenna pattern. Using this approach requires more complex antenna systems if very narrow beamwidth is desired. Therefore, it is important

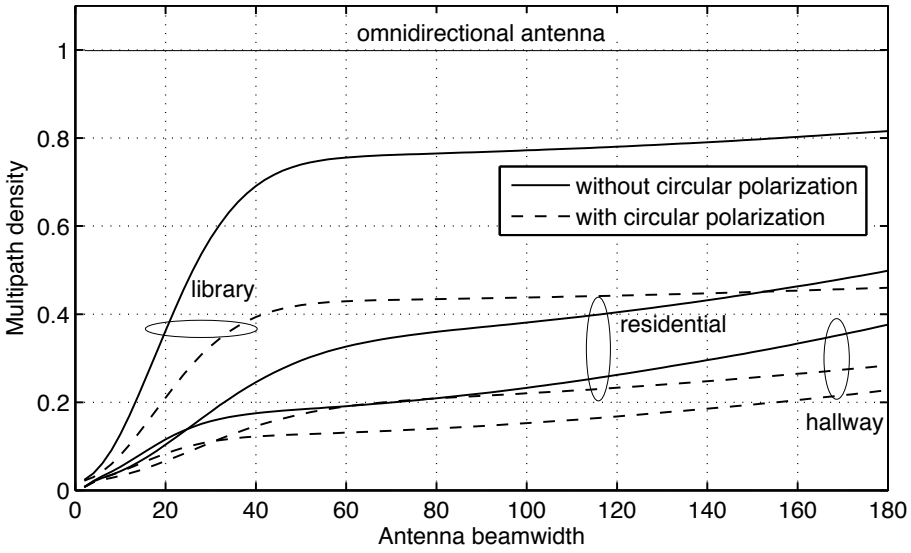

Figure 6.3: Multipath density with respect to antenna beamwidth for three of the five indoor scenarios described in [1] for 60 GHz wireless channel model. Multipath density is normalized to the interval of $[0, 1]$. Omnidirectional antennas are assumed to be operated with linear polarization and all possible paths are received at the receiver, resulting in a density of one.

to have the knowledge shown in Fig. 6.3 when designing the directional antenna for maximum efficiency.

In the next section, we use the derived statistics to analyze the directional behavior of different scenarios defined in the IEEE's channel model proposal and study the effects of directional transmission on the performance of communication systems.

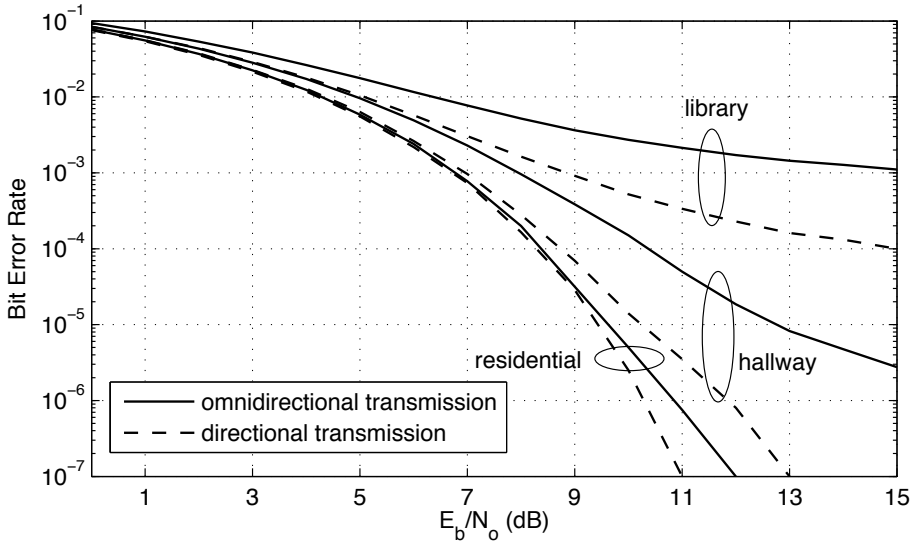

Figure 6.4: BER for three of the indoor scenarios defined by IEEE 802.15.3c. BPSK simulation is used to obtain the error rate curves. A square-root raised cosine filter with a roll-off factor of 0.3 is used. 2000 blocks are simulated with a block length of 200 and 20 samples per symbol. A uniform sectored antenna with beamwidth of 30^o and unit gain is assumed for both the transmitter and the receiver.

6.5.2 Performance analysis of the wireless system

One of the major performance metrics of a wireless system is the bit error rate, which depends on the level of ISI at the receiver. For high-speed communications in indoor environments, where both the transmitter and the receiver could be considered to be stationary, ISI is related to the number of multipaths and their individual power.

Fig. 6.4 compares the BER performance of a BPSK system in different LOS environments under directional and omnidirectional transmission scenarios. Some common blocks of a wireless communication system such as channel coding and

interleaving are not included so that we can clearly assess the impact of double-directional channel on the error rate of the raw data bits. We also assume a unit gain directional antenna in order to compare the effects of multipath reduction due to spatial filtering. For all scenarios, it is observed that directional transmission performs better than omnidirectional transmission in reducing the raw bit-error rates. In practical systems, directional antennas have much higher gain than the one simulated. Therefore, an even higher reduction in the error rate is expected due to the increased signal-to-noise ratio at the receiver. This allows the system to reduce the transmission power and still achieve the target error rate with directional transmission.

Compared with other scenarios, the residential environment has a very small delay spread of $0.1 - 0.2$ ns. Hence, the performance increase due to directional transmission is relatively limited. On the other hand, the library and hallway environments are severely affected by reflected paths and have a delay spread of a few ns. That is why a significant increase in performance is observed under directional transmission in these scenarios. One should note that, the relative difference between directional and omnidirectional transmission for multipath density (shown in Fig. 6.3) is much significant than the relative difference in error rate (shown in Fig. 6.4), specifically for the residential scenario. This is due to the very small delay spread in this specific environment.

6.6 Conclusion

We derived a double-directional channel model for 60 GHz directional wireless communications systems that includes the effects polarization. Based on the derived statistics of the angular parameters of the double-directional channel model, we further simplified the channel model for practical use. We also investigated the effects of antenna pattern on the multipath density, which can be used as a basis for performance and cost analysis. We integrated the effect of antenna beamwidth in the channel model based on assumptions that are validated for 60 GHz wireless communications. Using this model as a reference, we explored the error performance of 60 GHz wireless communications under directional transmission with different polarizations. The simulation results concur that in LOS environments, directional transmission with circular polarization reduces the multipath effect, and thus provides better performance than omnidirectional transmission, especially for systems operating at high data rates in dense multipath environments.

Bibliography

[1] S. Yong, "TG3c channel modeling sub-committee final report," *IEEE 802.15-07-0584-00-003c*, Jan. 2007 (https://mentor.ieee.org/802.15/file/07/15-07-0584-01-003c-tg3c-channel-modeling-sub-committee-final-report.doc).

[2] F. Yildirim, A. S. Sadri, and H. Liu, "Polarization effects for indoor wireless Communications at 60 GHz," *IEEE Commun. Lett.*, vol.12, no.9, pp.660-662, Sep. 2008.

[3] F. Yildirim and H. Liu, "A cross-layer neighbor discovery algorithm for directional 60 GHz networks," to appear in *IEEE Trans. Veh. Technol.*.

[4] N. Moraitis and P. Constantinou, "Indoor channel measurements and characterization at 60 GHz for wireless local area network applications," *IEEE Trans. Antennas Propagat.*, vol. 52, no. 12, pp. 3180–3189, Dec. 2004.

[5] J. Hubner, S. Zeisberg, K. Koora, J. Borowski and A. Finger, "Simple channel model for 60 GHz indoor wireless LAN design based on complex wideband measurements," in *Proc. IEEE VTC'97*, vol. 2, May 1997, pp. 1004–1008.

[6] T. Zwick, T. Beukema and H. Nam, "Wideband channel sounder with measurements and model for the 60 GHz indoor radio channel," *IEEE Trans. Veh. Technol.*, vol. 54, no. 4, pp. 1266–1277, Jul. 2005.

[7] D. Matic, H. Harada and R. Prasad, "Indoor and outdoor frequency measurements for MM-waves in the range of 60 GHz," in *Proc. IEEE VTC'98*, vol. 1, May 1998, pp. 567–57.

[8] J. Kunisch, E. Zollinger, J. Pamp and A. Winkelmann, "MEDIAN 60 GHz wideband indoor radio channel measurements and model," in *Proc. IEEE VTC'99*, vol. 4, Sep. 1999, pp. 2393–2397.

[9] A. Sadri, A. Maltsev, and A. Davydov, "IMST time-angular characteristics analysis," *IEEE 802.15-06-0141-00-003c*, Mar. 2006 (https://mentor.ieee.org/802.15/file/06/15-06-0141-01-003c-imst-time-angular-characteristics-analysis.ppt).

[10] A. Saleh and R. Valenzuela, "A statistical model for indoor multipath propagation," *IEEE J. Select. Areas Commun.*, vol. 5, no. 2, pp. 128–137, Feb. 1987.

[11] E. Skafidas, T. Pollock, K. Saleem, and C. Liu, "Channel measurements and setup for s-v channel model parameter determination." IEEE P802.15-05-0368-00-003c/r0, Jul. 2005.

[12] M. Steinbauer, A. F. Molisch, E. Bonek, "The double-directional radio channel," *IEEE Antennas and Propagat. Mag.,* vol. 43, no. 4, pp.51–63, Aug. 2001.

[13] K. Balakrishnan *et al.*, "Characterization of ultra wideband channels: small-scale parameters for indoor & outdoor office environments." IEEE 802.15-04-0342-00-004a, Jul. 2004.

[14] M. Steinbauer, "A comprehensive transmission and channel model for directional radio channels," COST259, No. TD(98)027. Bern, Switzerland, Feb. 1998.

[15] X. Hong, C.-X. Wang, B. Allen, and W. Q. Malik, "Correlation-based double-directional stochastic channel model for multiple-antenna ultra-wideband systems" *IET Proceedings Microwaves, Antennas & Propagation*, vol. 1, no. 6, pp. 1182–1191, Dec. 2007.

[16] A. Seyedi, "On the capacity of wideband 60GHz channels with antenna directionality," in *Proc. IEEE Globecom'07*, Nov. 2007, pp. 4532–4536.

Conclusions

We investigated the 60 GHz wireless channel and techniques for possible performance improvements and proposed several enhancements to already established standard. We utilize the unique characteristics of electromagnetic waves to overcome some of the limitations of the 60 GHz channel, and propose novel algorithms such as direction detection. In each case study, we support our proposals with solid analysis and numerical simulations and show that the proposed approaches improve the performance of the network relative to the current approaches.

In Chapter 2, we explored the error performance of 60 GHz wireless communications using different antenna polarizations. We first extended the channel impulse response model developed for 60 GHz wireless communications with linear polarization to incorporate the effects of circular polarization. We found that in LOS environments, circular polarization reduces the multipath effect, and thus provides better performance than linear polarization approach, especially for systems operating at high data rates. On the other hand, in NLOS environments, linear polarization should be used for optimum performance.

In Chapter 3, we proposed a topology detection algorithm in order to detect the presence or the absence of a direct path between the transmitter and the receiver in the 60 GHz channel. Such information can be employed for proper selection of polarization, which is discussed in Chapter 2. Using the derived throughput anal-

ysis, we have shown that the complexity introduced by the proposed algorithm is compensated by the increased efficiency due to the proper selection of polarization within the practical usage limits of indoor wireless systems.

In Chapter 4, we developed a neighbor-discovery algorithm for wireless communication networks with directional antennas operating in the 60 GHz band. This algorithm is a cross-layer scheme to effectively locate the neighbors around a device. It efficiently exploits the unique behaviors of different polarizations in LOS and NLOS environments for improved performance. Through the overhead and efficiency analysis, we have observed that even in highly populated and very dynamic networks, the time allocated for the neighbor-discovery algorithm does not exceed 10% in the worst-case scenario. Considering the significant increase in the physical-layer performance as a result of the efficient use of an appropriate polarization for each specific propagation scenario, this decrease in the network performance is expected to be compensated by the suppressed ISI and the reduced error rates.

In Chapter 5, we analyzed the direction-detection scheme that we introduced in Chapter 4 in a network environment. We statistically derive a relation for the events that might happen during the normal operation of the network that might require the re-detection of the direction of the receiver. We have shown that this re-detection does not clog the network by taking up too much time even in the extreme cases of a very crowded network and 100 events per second. We also derived a general expression for the normalized throughput of a network, which uses directional antennas on both ends of the communication channel. From the

BER and optimum data frame length analysis, we study the trend of the normalized throughput in a growing network of nodes. Based on this analysis, we can conclude that direction-detection will not be the bottleneck in the performance when a dynamic and growing network is considered.

In Chapter 6, we derived a double-directional channel model for 60 GHz wireless communications systems that includes the effects of directional antennas and polarization. Based on the derived statistics of the angular parameters of the double-directional channel model, we further simplified the channel model for practical use. We also investigated the effects of antenna pattern on the multipath density, which can be used as a basis for cost analysis. We integrated the effect of antenna beamwidth in the channel model based on our assumptions that are tailored for 60 GHz wireless communications. Using this model as reference, we explored the error performance of 60 GHz wireless communications under directional transmission. The simulation results concur that in LOS environments, directional transmission with circular polarization reduces the multipath effect, and thus provides better performance than omnidirectional transmission, especially for systems operating at high data rates.

Overall, this thesis provides improvements for the established standard IEEE 802.15.3c. One of the most significant follow-up research areas to this thesis is verifying the proposed algorithms and methods in the lab and supporting them with measurement data. Once verified with measurement results, the proposed modifications could be included in the standard.

APPENDICES

Appendix A – Detection Algorithm

Fig. A.1 shows the algorithm for the transmitter in the testing stage. The algorithm is initiated by a packet transmission request from the upper layer. If the packet is addressed to the receiver that was also the destination for the previous packet, the information from previous testing cycle could be used. If that is the case, the condition of successful delivery for the previous packet is checked. In either case, there will be an expiration time of the information that is obtained from the testing cycle: if the network topology is stationary, this time interval could be extended up to a maximum value of $t_{w,\max}$; when a failure of sending a packet occurs, or a when new destination is set, it will reset to a minimum value of $t_{w,\min}$. Based on these conditions, the algorithm either decides to use the previous information, or to start a new testing cycle.

The testing cycle is performed by sending a TEST frame in circular and linear polarization simultaneously (TEST(C) and TEST(L), respectively). This transmission is performed in an omni-directional manner to reach all directions. After this transmission, the transmitter sets back its mode to listening for potential ACK frames. If ACK/LOS is received from the receiver, transmitter switches to circular mode and initiates the direction-finding algorithm; if ACK/NLOS is received from the receiver, the transmitter switches to linear mode and initiates the direction-finding algorithm.

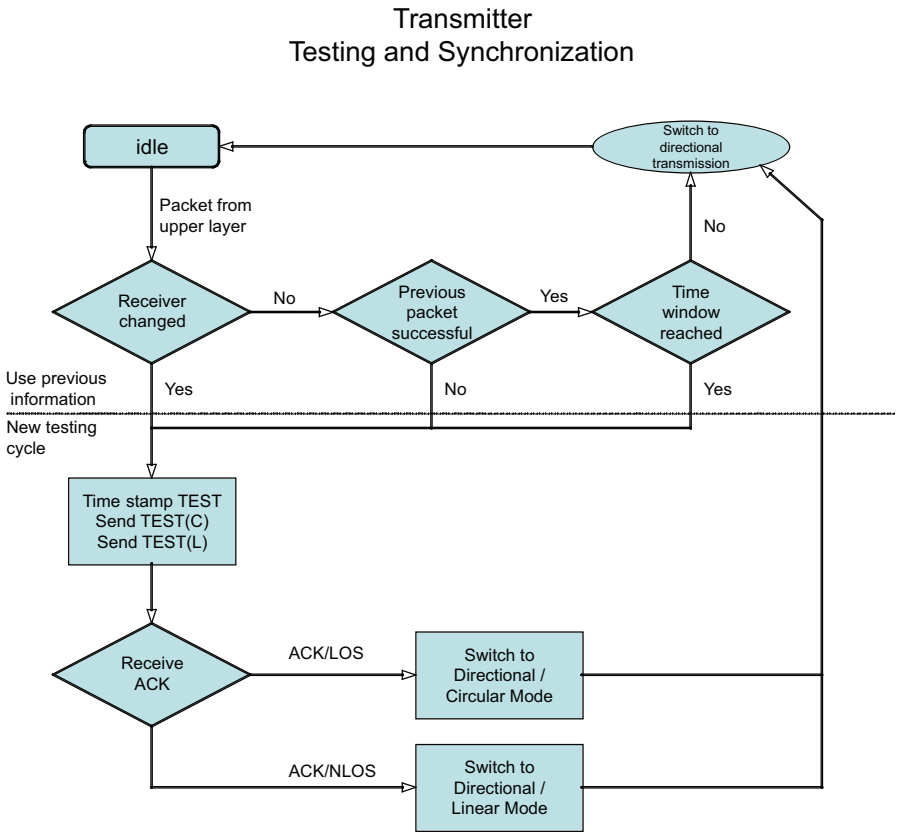

Figure A.1: Flowchart - transmitter in testing stage.

Fig. A.2 shows the algorithm at the receiver in the testing cycle. The cycle is initiated when a TEST frame is received from lower level. The pseudo-synchronization process requires synchronization of the internal clock of the receiver with the timestamp on the most dominant path. Recall that the dominant path will be the first received path in the case of LOS, and the strongest one in the case of NLOS. Therefore, if NLOS is determined after comparison of TEST frames, the receiver keeps track of the magnitude of the received paths to determine the strongest one, and keeps updating the synchronization each time a stronger path

is received.

Once the receiver determines the topology of the network and sends this information back to the transmitter, it initiates the direction finding and data transmission cycle shown in Fig. A.3. Each frame sent out of the transmitter is time stamped. The transmitter starts to send out directional RTS frames from an initial sector and cycles all sectors in a cyclic manner. Failure to receive a CTS from the receiver for a specific period of time in each sector triggers the transmitter to advance to the next sector. If all sectors are probed with RTS and still no response from the transmitter is received, the packet is dropped.

In the data-transmission and direction-finding stage, the receiver executes an algorithm fairly similar to existing data transmission algorithms; the only major difference is that, as shown in Fig. A.4, the timestamp of each received frame is compared with the internal clock of the receiver. If they match, a reply will be sent to the transmitter to indicate that the sector it uses is the most efficient direction for communication; otherwise, the received frame is discarded.

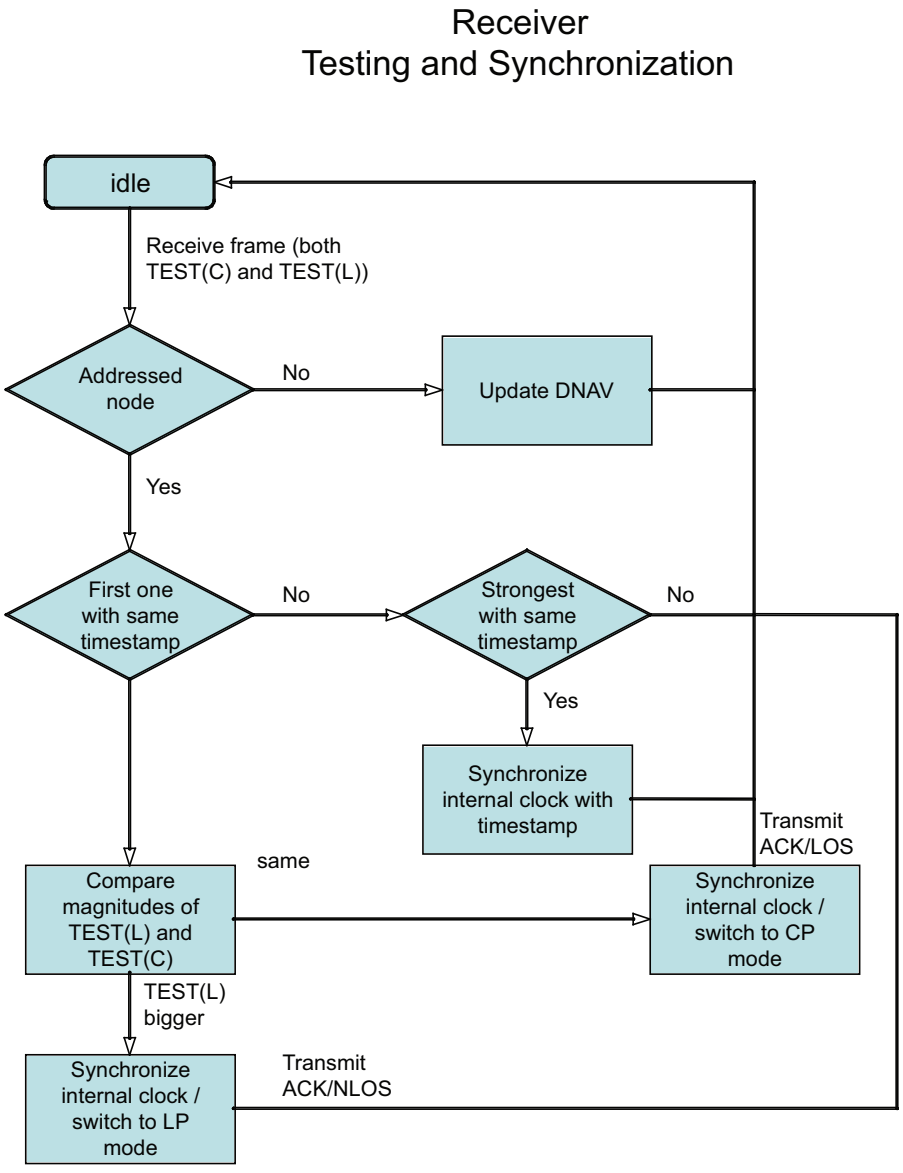

Figure A.2: Flowchart - receiver in testing stage.

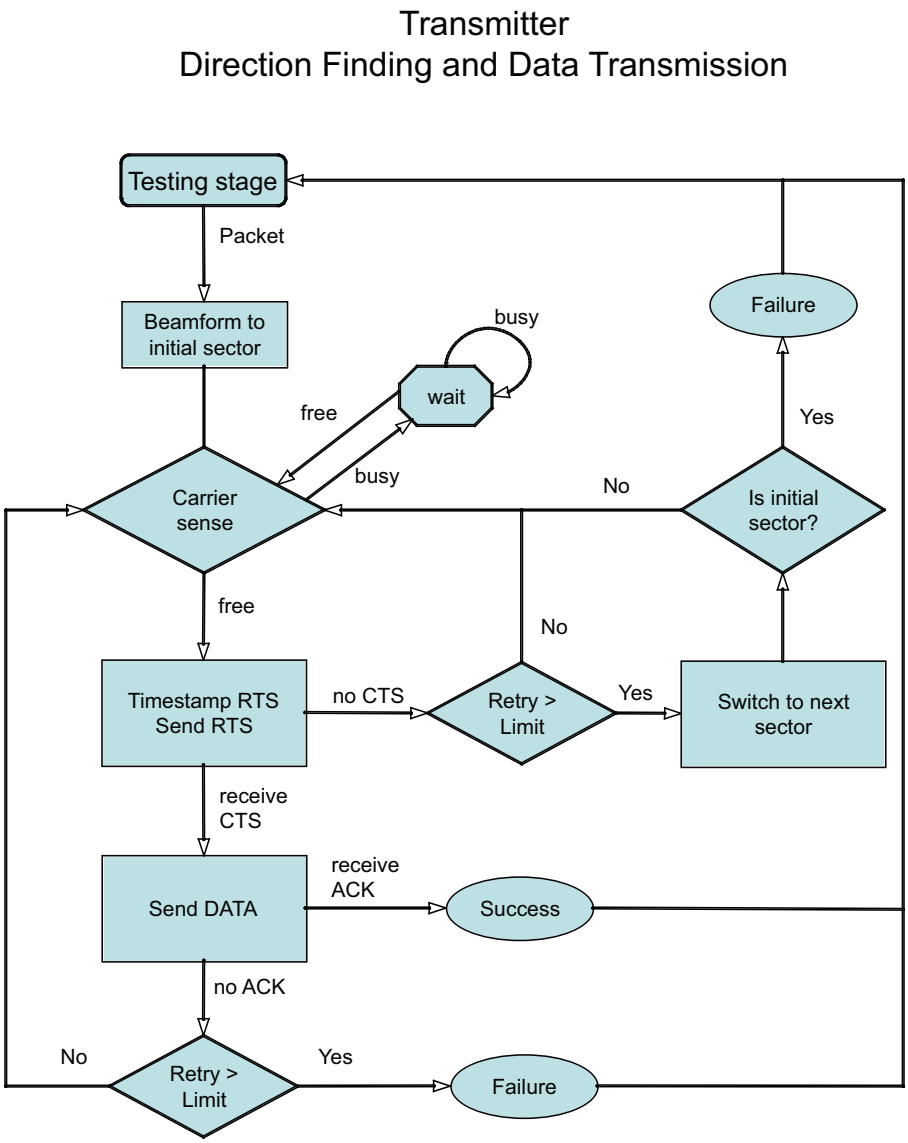

Figure A.3: Flowchart - transmitter in direction-finding stage.

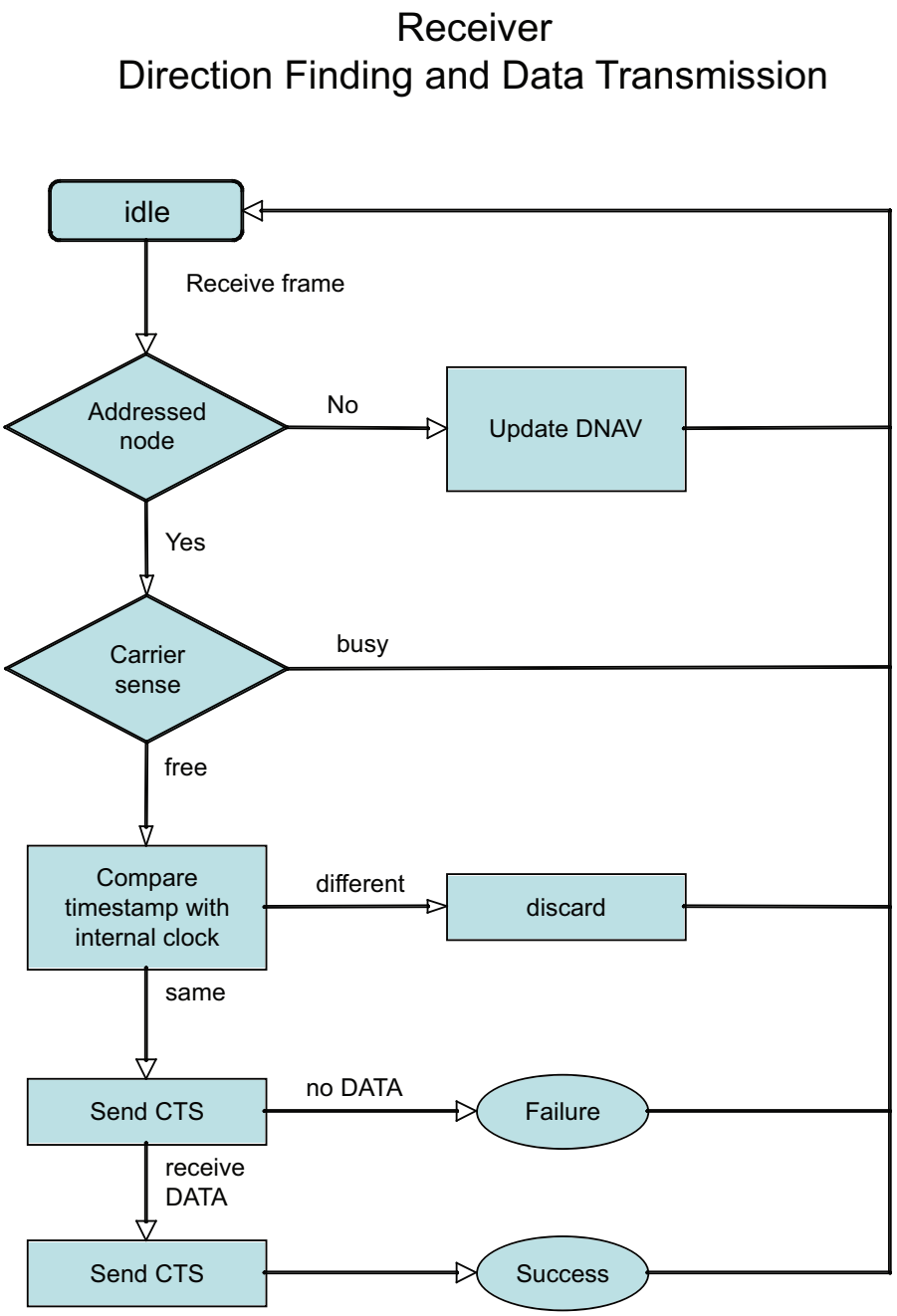

Figure A.4: Flowchart - receiver in direction-finding stage.

Bibliography

[1] P. F. M. Smulders, "Exploiting the 60 GHz band for local wireless multimedia access: prospects and future directions," *IEEE Commun. Mag.*, vol. 40, pp. 140–147, Jan. 2002.

[2] F. Giannetti, M. Luise, and R. Reggiannini, "Mobile and personal communications in 60 GHz band: A survey," *Wirelesss Personal Comunications*, vol. 10, pp. 207–243, 1999.

[3] R. C. Daniels and R. W. Heath, Jr., "60 GHz Wireless Communications: Emerging Requirements and Design Recommendations," *IEEE Vehicular Technology Magazine*, vol. 2, no. 3, pp. 41-50, Sep. 2007.

[4] P. Smulders, "Broadband wireless LANs: a feasibility study" PhD Thesis, Eindhoven Univeristy of Technology, The Netherlands, ISBN 90-386-0100-X, 1995.

[5] P. F. M. Smulders and A. G. Wagemans, "Wideband Indoor Radio Propagation Measurements at 58 GHz," *IEE Elect. Lett.*, vol. 28, no. 13, pp. 1270–1271, 1992.

[6] P. F. M. Smulders and G. J. A. P. Vervuurt, "Influence of Antenna Radiation Patterns on Mm-wave Indoor Radio Channels," Intl. Conf. Univ., Pers. Commun., Ottawa, Canada, pp. 631–635, Oct. 1993.

[7] S. Yong, "TG3c channel modeling sub-committee final report," *IEEE 802.15-07-0584-00-003c*, Jan. 2007 (https://mentor.ieee.org/802.15/file/07/15-07-0584-01-003c-tg3c-channel-modeling-sub-committee-final-report.doc).

[8] IEEE. Std. 802.15.3-2003 ed. Wireless Medium Access Control (MAC) and Physical Layer (PHY) Specifications for High Rate Wireless Personal Area Networks (WPANs).

[9] A. Sadri, "802.15.3c Usage Model Document (UMD), Draft," 15-05- 0055-21-003c, Jan. 2007 (ftp://ieee:wireless@ftp.802wirelessworld.com/15/06/15-06-0055-21-003c-mmwave-802-15-3c-usage-model-document.doc)

[10] A. Saleh and R. Valenzuela, "A statistical model for indoor multipath propagation," *IEEE J. Select. Areas Commun.*, vol. 5, no. 2, pp. 128–137, Feb. 1987.

[11] J. Foerster, "Path loss proposed text and S-V model information." IEEE P802.15-02380r0-SG3a, Jun. 2002.

[12] A. F. Molisch, U. G. Schuster, and C. C. Chong, "Measurement procedure and methods on channel parameter extraction." IEEE 15-04-283-00-4a, May 2004

[13] K. Balakrishnan *et al.*, "Characterization of ultra wideband channels: small-scale parameters for indoor & outdoor office environments." IEEE 802.15-04-0342-00-004a, July 2004.

[14] H. Xu, V. Kukshya and T. Rappaport, "Spatial and temporal characteristics of 60-GHz indoor channels," *IEEE J. Select. Areas Commun.*, vol. 20, no. 3, pp. 620–630, Apr. 2002.

[15] A. Bourdoux, J. Nsenga, W. Van Thillo, F. Horlin and L. Van der Perre, "Air interface and physical layer techniques for 60 GHz WPANs," in *Proc. Int. Symp. on Comm. and Veh. Tech.*, Nov. 2006, pp. 1–6.

[16] H. Kim, K. Ahn and H. Baik, "Phase noise suppression algorithm for OFDM-based 60 GHz WLANs," in *Proc. Int. ISWPC*, Jan. 2006, pp. 4.

[17] T. Chen, H. Zhang and I. Chlamtac, "High speed orthogonal waveform based indoor wireless transmission by an UWB and 60 GHz dual band system," in *Proc. ISWCS'06*, Sep. 2006, pp. 423–427.

[18] H. El Ghannudi, L. Clavier, A. Bendjaballah, A. Boe and P. Rolland, "Performance of IR-UWB at 60 GHz for ad hoc networks with directive antennas," in *Proc. IEEE ICUWB'06*, Sep. 2006, pp. 149–154.

[19] S. Pinel, I. Kim, K. Yang and J. Laskar, "60 GHz linearly and circularly polarized antenna arrays on liquid crystal polymer substrate.," in *Proc. Euro. Microwave Conf.*, Sep. 2006, pp. 858–861.

[20] S. Lei, S. Houjun, L. Deng and C. Yong, "Study of the improved mm-wave omni-directional microstrip antenna," in *Proc. ISAPE'06*, Oct. 2006, pp. 1–4.

[21] B. Langen, G. Lober and W. Herzig, "Reflection and transmission behaviour of building materials at 60 GHz," in *Proc. IEEE PIMRC'94*, vol. 2, Sep. 1994, pp. 505–509.

[22] K. Sato, *et al.* "Measurement of reflection and transmission characteristics of interior structures of office building in the 60-Ghz band," *IEEE Trans. Antennas Propagat.*, vol. 45, pp. 1783–1791, Dec. 1997.

[23] N. Moraitis and P. Constantinou, "Measurements and characterization of wideband indoor radio channel at 60 GHz," *IEEE Trans. Wireless Commun.*, vol. 5, no. 4, pp. 880–889, Apr. 2006.

[24] J. Hubner, S. Zeisberg, K. Koora, J. Borowski and A. Finger, "Simple channel model for 60 GHz indoor wireless LAN design based on complex wideband measurements," in *Proc. IEEE VTC'97*, vol. 2, May 1997, pp. 1004–1008.

[25] T. Zwick, T. Beukema and H. Nam, "Wideband channel sounder with measurements and model for the 60 GHz indoor radio channel," *IEEE Trans. Veh. Technol.*, vol. 54, no. 4, pp. 1266–1277, Jul. 2005.

[26] D. Matic, H. Harada and R. Prasad, "Indoor and outdoor frequency measurements for MM-waves in the range of 60 GHz," in *Proc. IEEE VTC'98*, vol. 1, May 1998, pp. 567–57.

[27] J. Kunisch, E. Zollinger, J. Pamp and A. Winkelmann, "MEDIAN 60 GHz wideband indoor radio channel measurements and model," in *Proc. IEEE VTC'99*, vol. 4, Sep. 1999, pp. 2393–2397.

[28] A. Sadri, A. Maltsev, and A. Davydov, "IMST time-angular characteristics analysis," *IEEE 802.15-06-0141-00-003c*, Mar. 2006 (https://mentor.ieee.org/802.15/file/06/15-06-0141-01-003c-imst-time-angular-characteristics-analysis.ppt).

[29] F. Yildirim and H. Liu, "Directional MAC for 60 GHz using polarization diversity extension (DMAC-PDX), *in Proc. IEEE Globecom07*, Nov. 2007.

[30] Federal Communications Commission, "Amendment of parts 2, 15 and 97 of the commissions rules to permit use of radio frequencies above 40 GHz for few radio applications," *FCC 95-499*, ET Docket No. 94-124, RM- 8308, Dec. 15, 1995.

[31] C. J. Gibbins, "Radiowave propagation in the 30-60 GHz band," *IEE Colloquium Radiocomm. in the Range 30-60 GHz*, pp. 1/1-1/4, Jan. 1991.

[32] C. Koh, "The benefits of 60 GHz unlicensed wireless communications," *YDI Wireless White Paper 041104A*, Nov. 2003.

[33] M. Marcus and B. Pattan, "Millimiter wave propagation: spectrum management implications," *IEEE Microwave Mag.*, pp. 54–62, Jun. 2005.

[34] A. J. Richardson and P. A. Watson, "Use of the 55–65 GHz oxygen absorption band for short-range broadband radio networks with minimal regulatory control," *IEE Proceedings*, vol. 137, no. 4, Aug. 1990.

[35] F. Yildirim, A. S. Sadri, and H. Liu, "Polarization effects for indoor wireless Communications at 60 GHz," *IEEE Commun. Lett.*, vol.12, no.9, pp.660-662, Sep. 2008.

[36] RadioPlan RPS simulator, http://www.rps.com

[37] C. A. Balanis, *Advanced engineering electromagnetics*. New York: Wiley, 1989.

[38] I. Katz, "Radar reflectivity of the ocean surface for circular polarization," *IEEE Trans. Antennas Propagat.*, vol. 11, pp. 451–453, Jul. 1963.

[39] K. Sato, *et al.* "Measurement of reflection and transmission characteristics of interior structures of office building in the 60-Ghz band," *IEEE Trans. Antennas Propagat.*, vol. 45, pp. 1783–1791, Dec. 1997.

[40] Naval Air Systems Command "Electronic warfare and radar systems engineering handbook," Washington DC, Apr. 1997.

[41] M. Paulson, S. O. Kundukulam, C. K. Aanandan, and P. Mohanan, "A new compact dual-band dual-polarized microstrip antenna," *Microwave and Optical Technol. Lett.*, vol. 29, no. 5, pp. 315–317, 2001.

[42] W. C. Chan, *Performance analysis of telecommunications and local area networks*. Norwell: Kluwer Academic Publishers, 1999.

[43] Y. Xiao, X. Shen, and H. Jiang, "Optimal ACK mechanisms of the IEEE 802.15.3 MAC for ultra-wideband systems," *IEEE J. Select. Commun.*, vol. 24, no. 4, pp. 836–842, Apr. 2006.

[44] S. Geng, *et al.* "Millimeter-wave propagation channel characterization for short-range wireless communications," *IEEE Trans. Veh. Technol.* , vol.58, no.1, pp.3–13, Jan. 2009.

[45] T. Manabe, *et al.* "Polarization dependence of multipath propagation and high-speed transmission characteristics of indoor millimeter-wave channel at 60 GHz ," *IEEE Trans. Veh. Technol.*, vol. 44, no. 2, pp. 268–274, May 1995.

[46] A. Xueli and R. Hekmat, "Directional MAC protocol for millimeter wave based wireless personal area networks," in *Proc. IEEE VTC-Spring 2008*, May 2008, pp. 1636–1640.

[47] F. Kojima, C. W. Pyo, Z. Lan, H. Harada, S. Kato, and H. Nakase, "Necessary modifications on conventional IEEE802.15.3b MAC to achieve IEEE802.15.3c millimeter wave WPAN," in *Proc. IEEE PIMRC 2007*, Sep. 2007, pp. 1–5.

[48] R. R. Choudhury, X. Yang, R. Ramanathan, and N. H. Vaidya, "Using directional antennas for medium access control in ad hoc networks," in *Proc. ACM MobiCom*, Sep. 2002, pp. 59–70.

[49] N. S. Fahmy, T. D. Todd, and V. Kezys, "Ad hoc networks with smart antennas using IEEE 802.11-based protocols", in *Proc. IEEE Int. Conf. Commun.*, Apr. 2002, pp. 3144–3148.

[50] Y.-P. Hong, J.-M. Kim, S.-C. Jeong, D.-H. Kim, and J.-G. Yook, "Low-profile S-band dual-polarized antenna for SDARS application," *Antennas and Wireless Propagat. Lett.*, vol. 4, pp. 475–477, Jan. 2005.

[51] J. Jansson, A. Mantyniemi and J. Kostamovaara, "A delay line based CMOS time digitizer IC with 13 ps single-shot precision," in *Proc. IEEE ISCAS'05*, May 2005, pp. 4269–4272.

[52] Z. Zhang, "Performance of neighbor discovery algorithms in mobile ad hoc self-configuring networks with directional antennas," in *Proc. IEEE MILCOM*, Oct. 2005, pp. 3162–3168.

[53] F. Yildirim and H. Liu, "A cross-layer neighbor discovery algorithm for directional 60 GHz networks," to appear in *IEEE Trans. Veh. Technol.*, 2009.

[54] N. Moraitis and P. Constantinou, "Indoor channel measurements and characterization at 60 GHz for wireless local area network applications," *IEEE Trans. Antennas Propagat.*, vol. 52, no. 12, pp. 3180–3189, Dec. 2004.

[55] E. Skafidas, T. Pollock, K. Saleem, and C. Liu, "Channel measurements and setup for s-v channel model parameter determination." IEEE P802.15-05-0368-00-003c/r0, Jul. 2005.

[56] M. Steinbauer, A. F. Molisch, E. Bonek, "The double-directional radio channel," *IEEE Antennas and Propagat. Mag.,* vol. 43, no. 4, pp.51–63, Aug. 2001.

[57] M. Steinbauer, "A comprehensive transmission and channel model for directional radio channels," COST259, No. TD(98)027. Bern, Switzerland, Feb. 1998.

[58] X. Hong, C.-X. Wang, B. Allen, and W. Q. Malik, "Correlation-based double-directional stochastic channel model for multiple-antenna ultra-wideband systems" *IET Proceedings Microwaves, Antennas & Propagation*, vol. 1, no. 6, pp. 1182–1191, Dec. 2007.

[59] A. Seyedi, "On the capacity of wideband 60GHz channels with antenna directionality," in *Proc. IEEE Globecom'07*, Nov. 2007, pp. 4532–4536.